# A STUDY TO VERIFY THE MATERIAL SURFACE CONCEPT OF WATER TABLE BY EXAMINING ANALYTICAL AND NUMERICAL MODELS

A Thesis

by

SIREESH KUMAR DADI

Submitted to the Office of Graduate Studies of
Texas A&M University
in partial fulfillment of the requirements for the degree of

MASTER OF SCIENCE

August 2010

Major Subject: Geology

# A STUDY TO VERIFY THE MATERIAL SURFACE CONCEPT OF WATER TABLE BY EXAMINING ANALYTICAL AND NUMERICAL MODELS

A Thesis

by

SIREESH KUMAR DADI

Submitted to the Office of Graduate Studies of
Texas A&M University
in partial fulfillment of the requirements for the degree of

MASTER OF SCIENCE

Approved by:

| | |
|---|---|
| Co-Chairs of Committee, | Hong-Bin Zhan |
| | David Sparks |
| Committee Member, | Yuefeng Sun |
| Head of Department, | Andreas Kronenberg |

August 2010

Major Subject: Geology

# ABSTRACT

A Study to Verify the Material Surface Concept of Water Table by Examining Analytical and Numerical Models. (August 2010)

Sireesh Kumar Dadi, B.Tech, Indian Institute of Technology, Guwahati

Co-Chairs of Advisory Committee: Dr. Hong-Bin Zhan
Dr. David Sparks

The highly nonlinear nature of unsaturated flow results in different ways to approximate the delayed or instantaneous movement of the water table. In nearly all the approaches, the water table is conceptually treated as a "material surface". This term defines the water table as having two simultaneous properties: 1) the pressure along the surface is atmospheric pressure, and 2) the water table is fixed to the material, i.e., a set of water particles. This article makes an attempt to explain that the water table, defined as the surface at atmospheric pressure, is not a material boundary, and the water table can move independent of the water particles.

Velocity of the water table and velocity of drainage are compared with three analytical models: the Neuman model, which assumes instantaneous drainage from the unsaturated zone; the Moench model, which considered gradual drainage from the unsaturated zone using a series of exponential terms in the water table boundary condition; and the Mathias-Butler model, which obtained a new drainage function based on a linearized Richard's equation but limited the variation of soil moisture and hydraulic conductivity in the unsaturated zone to exponential functions. Numerical

analysis was conducted with VS2DT and both the numerical and the analytical results were compared with a 7-day, constant rate pumping test conducted by University of Waterloo researchers at Canadian Air Force Base Borden in Ontario, Canada.

## ACKNOWLEDGEMENTS

I owe a debt of gratitude to many people who supported the completion of this study, my interest in geology, and my education. I am especially grateful for the guidance of my advisor, Dr. Hongbin Zhan, who encouraged the exploration of my interests and then directed me in new research directions. Dr. Yuefeng Sun, a greatly appreciated committee member, offered valuable insights and taught me many lessons, the least of which was the value of a concise, elegant argument. I am also thankful for the assistance of Dr. David Sparks, who encouraged me to better understand the concept of water table and the highly insightful comments in dealing with the water table boundary condition.

I could never fully express my thanks to my friends, colleagues, and teachers in the Department of Geology and Geophysics, who made my time at Texas A&M both productive and happy. Thanks go to Bharat, Vivek, Sandeep and Ahmed for friendship and thesis advice. Thanks are due to Marathon Oil/Questar Corporation for their financial support of my education. I extend my gratitude to Texas Higher Education Board for partially supporting my research through the Advanced Research Program. I would like to thank Allen F. Moench for providing the FORTRAN code, WTAQ4, and insight into some of the challenges with VS2DT. I am also thankful to Dr Anthony Endres for providing the field aquifer test data from Borden Site, Canada.

Finally, thanks to my family: Jagadamba and Narayana Dadi, my parents, and my sister, Swathi, for their constant and overwhelming support.

# TABLE OF CONTENTS

# LIST OF FIGURES

FIGURE Page

# LIST OF TABLES

# 1. INTRODUCTION AND LITERATURE REVIEW

The concept of the water table has always been only a useful approximation to the more complex boundary condition between the saturated and the unsaturated regions. Existing saturated flow theories are built upon the water table concept, yet how the water table responds when the hydrological conditions change is still one of the fundamental unanswered questions in hydrological sciences. In reality, flow in the unsaturated zone is described by a nonlinear governing equation, in which hydraulic conductivity and specific moisture capacity are functions of water content. Such a governing equation is very difficult to solve analytically, and numerical simulations are almost always needed. Analytical solutions are more desirable for a number of practical issues such as aquifer parameter estimation. Therefore, for many years, hydrologists have focused on saturated flow, which is much easier to solve analytically. This approximate model requires a condition that defines the moving upper boundary of the saturated zone: this artificial boundary is the water table. In this study, water table is defined as the surface where pore pressure equals atmospheric pressure, and drainage velocity is defined as the velocity of the water particles on the water table defined by Darcy's velocity. This definition of water table is consistent with comments made by *Holzer* [2009] by decoupling relationship between fluid pressure and saturation. According to *Holzer* [2009] the top of the zone of saturation may be above, at or below the water table surface.

---

This thesis follows the style of *Water Resources Research.*

The motion of the water table was approximated either as a delayed or instantaneous drainage boundary condition by different analytical models including *Boulton* [1954, 1963], *Dagan* [1967], *Neuman* [1972, 1974], *Bear* [1972], *Moench* [1997, 2008] and *Mathias and Butler* [2006]. In nearly all these approaches, the water table is conceptually treated as a material surface. This term defines the water table as a surface attached to a set of particles. If the water table is a material surface, the speed of its movement will be limited by the speed of the water movement, which is subsequently controlled by Darcy's law. Figure 1 demonstrates the movement of the water table with respect to the surface where saturation equals 1 during a pumping test. The water table surface coincides with the surface where saturation equals 1 before the initiation of pumping and at steady state. But as the pumping starts, due to the sudden change in pressure around the pumping well, the water table surface drops faster than the water particles attached to it. The faster movement of the water table compared to the water particles on it questions the assumption of water table surface being a material surface.

*Boulton* [1954, 1963] introduced one delay index, $\alpha$, that accounted for the vertical leakage through an aquitard, which had a free surface, but did not consider vertical flow in the unsaturated zone. *Neuman* [1972, 1974] and *Dagan* [1967] models accounted for vertical flow and anisotropy in the saturated zone, but ignored drainage from unsaturated zone to the water table. *Kroszynski and Dagan* [1975] presented an analytical model using the *Richards* [1931] equation, assuming the unsaturated zone was

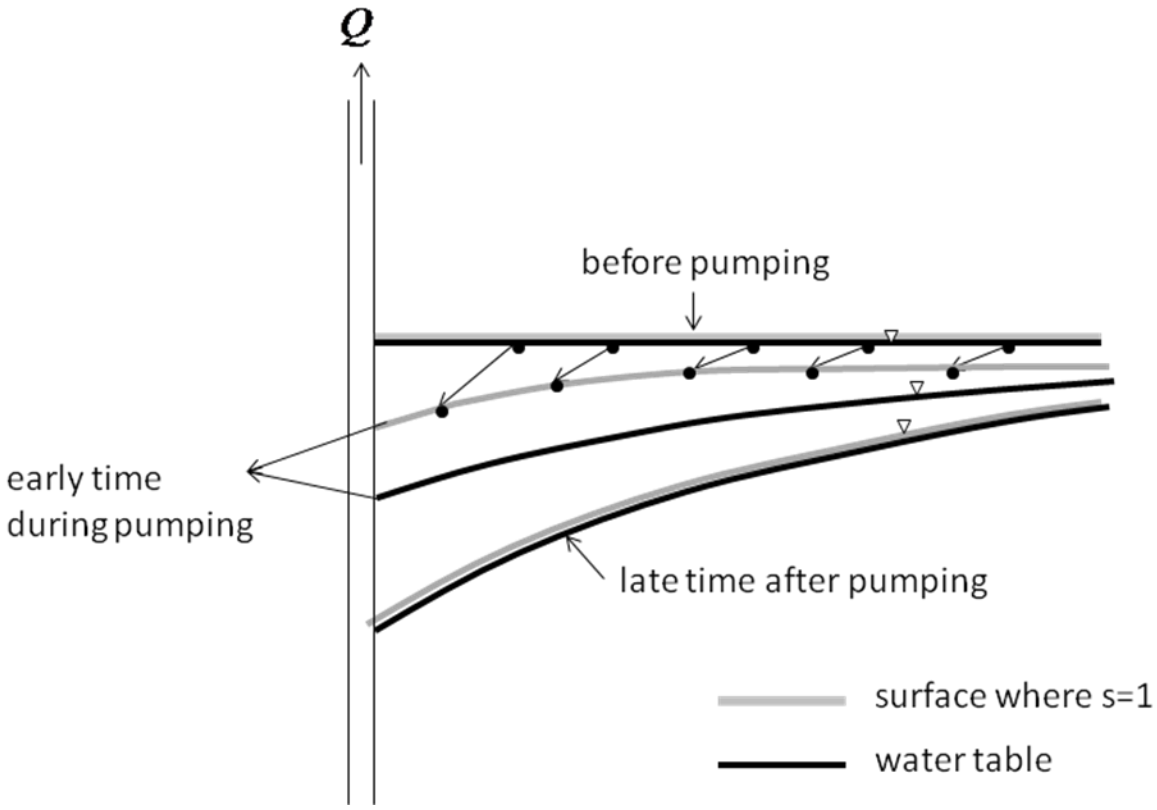


Figure 1: Schematic showing movement of the water table and the water particles on it.

infinitely deep, where soil moisture and hydraulic conductivity were expressed as exponential functions of the pressure head. Both *Kroszynski and Dagan* [1975] and *Dagan* [1967] assumed a rigid aquifer and linearized the nonlinear water table boundary condition, which implied that the solution was valid only when the water table drawdown was small compared to the saturated zone thickness. *Neuman* [1972, 1974] model was widely accepted by the groundwater community due to the relatively fewer assumptions. *Hunt and Scott* [2005] reviewed the equations that lead to the Theis, Hantush-Jacob, and Boulton solutions for unsteady flow to a pumped well. It shows that the Boulton solution contained both the Theis and Hantush-Jacob solutions as special cases. The regions of overlap among these solutions were obtained and the Boulton solution was extended to a layered system.

*Nwankor et al.* [1984] calculated specific yield of an unconfined sand aquifer by pumping test type-curves, volume balance and laboratory drainage tests. *Nwankor et al.* [1984], similar to *Bear* [1972], observed a gradually increasing transient specific yield with the volume balance approach and the specific yield closely approached the laboratory determined value. The underestimation of specific yield values obtained from type-curve analysis using *Neuman* [1972] and *Boulton* [1963] models explained the need for better representation of the delayed drainage from above the water table. *Nwankor et al.* [1992] demonstrated that delayed drainage of soil water above water table explained the relatively small values of specific yield derived from pumping test type-curves. *Duke* [1972] observed the nonlinear relationship between volume of water released and the shallow water table fluctuation.

*Nachabe* [2002], based on the earlier work of *Duke* [1972], introduced a closed-form analytical expression for specific yield, which was dependent on time and depth to water table (DTWT). In a field study at Florida, *Said et al.* [2005] demonstrated a methodology to estimate the specific yield and soil properties in shallow water environments using continuous soil moisture data. In addition to porosity and soil specific retention, the specific yield is expressed as a function of DTWT, pore-size distribution index and soil air entry pressure head of the Brooks and Corey water retention model [*Brooks and Corey*, 1964]. Assumptions of this model included equilibrium status in terms of water table elevation and a homogeneous soil profile. Evapotranspiration in the day and replenishment in the night may not justify hydrostatic water content distribution all the times [*Said et al.*, 2005]. The change in specific yield for rising and falling water table was not included in the model. Difference between the specific yield for wetting and drying decreased significantly with depth.

*Narasimhan and Zhu* [1993] developed a numerical model and concluded the importance of drainage from the unsaturated zone and that exponential drainage was an oversimplification of the drainage process. Following the experimental findings from *Narasimhan and Zhu* [1993] and *Nwankor et al.* [1992], *Moench* [1994] substituted the Boulton convolution integral [*Boulton*, 1954, 1963] for the Neuman water table boundary condition [*Neuman*, 1972, 1974]. The Laplace transform solution with the revised delay index reduced the discrepancy between the measured and analytical drawdowns especially in piezometers located near the water table. The discrepancy was not completely eliminated because the Boulton's convolution integral did not accurately

describe the drainage process [*Narasimhan and Zhu*, 1993]. *Moench* [1997] by accounting for wellbore storage extended the validity of the Laplace transform solution [*Moench*, 1995] to calculate specific storage and other unconfined aquifer parameters from pumping-well data. *Moench et al.*, [2001] was among the first few to use the parameter estimation algorithm to analyze the USGS Cape Cod, Massachusetts pumping test to obtain the saturated zone hydraulic characteristics. *Moench* [2004] suggested that using three empirical constants in the boundary condition gave a better fit between measured and simulated drawdowns in the complete time range. *Moench* [2004] found that instead of using late time data for which the pumping test had to be performed for long time, an accurate time-varying drainage model and piezometer data can give an optimized result. Of concern was the variability of the empirical constants for different aquifer tests and the unaccountability of the unsaturated zone. Further investigation for coupling to the unsaturated zone was done by *Mathias and Butler* [2006] by following the work of *Kroszynski and Dagan* [1975] based on the linearized Richards equation. *Moench* [2004] made an attempt to calculate large scale soil moisture characteristics from a detailed unconfined aquifer test conducted by *Bevan* [2002] at Borden site in Canada. The aquifer test parameters were estimated using WTAQ4 which was coded to incorporate instantaneous drainage *Neuman* [1972, 1974] model, *Moench* [2004] model and *Mathias and Butler* [2006] model. Results obtained by running parameter estimation with USGS numerical model VS2DT together with soil function relations by *Brooks and Corey* [1964] and *Assouline* [2001] demonstrated a rapid decline in relative hydraulic conductivity (RHC) at field-scale compared to core-scale.

## 2. OBJECTIVES

The objective of this work is to prove that the water table, defined as the surface where pore pressure is atmospheric pressure, is not a material boundary, and it can move faster than water particles; therefore flow in the unsaturated zone must be considered to correctly interpret the pumping test data in an unconfined aquifer.

The Nueman, Moench and Mathias-Butler models for unconfined aquifer test analysis and the USGS numerical model VS2DT will be revisited to explain that the water table is not a material boundary. The water table positions at different times will be determined to calculate speed of the water table. The speed of the water table movement will be compared against the water particle movement calculated by Darcy's law to test the material free surface concept and the proposed water table boundary conditions of *Boulton* [1954], *Bear* [1972], *Neuman* [1972] and *Moench* [2004]. The field pumping test data collected at the Borden site will be reinterpreted with numerical simulations and emphasis on the importance of properly incorporating the unsaturated flow into the pumping test interpretation in unconfined aquifers will be discussed. Using insight from the numerical models and the pumping test data, a list of conditions, in terms of aquifer and well properties and pumping rates, to identify the conditions under which water table boundary concept can be reasonably applied, and under what conditions a fully variably saturated flow model is required.

# 3. METHODOLOGY

## 3.1 Aquifer test analysis

This study is based on an extensively monitored seven day continuous pumping rate aquifer test conducted in an unconfined aquifer in Canadian Forces Base Borden, Ontario [*Bevan et al.,* 2005]. The unconfined aquifer has a glacio-deltaic or glacio-fluvial origin with local heterogeneity consisting of discontinuous lenses and beds of fine-, medium- and, coarse- grained sand. There are also infrequent silt, silty-clay, and coarse sand layers. The zone of fluctuations of the water table varies seasonally by 1.0 m interval. During a tracer test conducted in August 1982, hydraulic heads were monitored using an array of piezometers situated at various depths. The hydraulic head field at the tracer site is relatively smooth and uniform. The annual mean magnitude and orientation of the hydraulic gradient is estimated to be about 4.3E-5 m/sec and N45E, respectively. The average vertical gradient appears to be downward on the basis of the vertical movement of tracer plume, but its value is so small that its detection is difficult using multilevel piezometers [*Sudicky*, 1986]. The aquifer is 9 m thick underlain by clayey silt material. Data suggested the initial water table in August 2001 at the aquifer site is 2.75 m below the ground surface leaving 6.25 m saturated zone. Further information about the geology of the aquifer can be found in *Sudicky* [1986], *Bevan* [2002] and *Bevan et al.* [2005]. The monitoring system involved 11 pressure transducer wells, 31 wells using an electrical acoustic sounder with measurements made twice daily and 6 neutron access tubes. Most of the observation wells are screened over the lower 0.35 m [*Bevan et al.*,

2005], and the diameter of the observation wells in the study are 0.35 m consistent with the approximation made by *Moench* [2008]. Although all the pressure transducer observation well drawdown measurements are analyzed, 4 pairs of them at 1.5 m, 3 m, 5 m and 15 m are used extensively to obtain both the vertical ground water velocity and the velocity of the water table (i.e. surface at atmospheric pressure). Figure 2 displays a plan view of the Borden test site showing the positions of the pumping well, the piezometers with transducers, the piezometers measured by hand, and the neutron access tubes. Figure 3 shows a vertical cross-section along the southern transect.

The pumping well was screened over the bottom 3.75 m of the aquifer with an internal diameter of 0.13 m. The pumping well PW1 was pumped continuously for 7 days at the rate of 40 L/min. The pumping rate was monitored at regular intervals by calculating the time required to fill a container. Table 1 shows the details about the radial distance and the depth of the observation wells from the pumping well. Further information on the location and details of the observation wells and neutron probes can be obtained from *Bevan et al.* [2005] and *Moench* [2008].

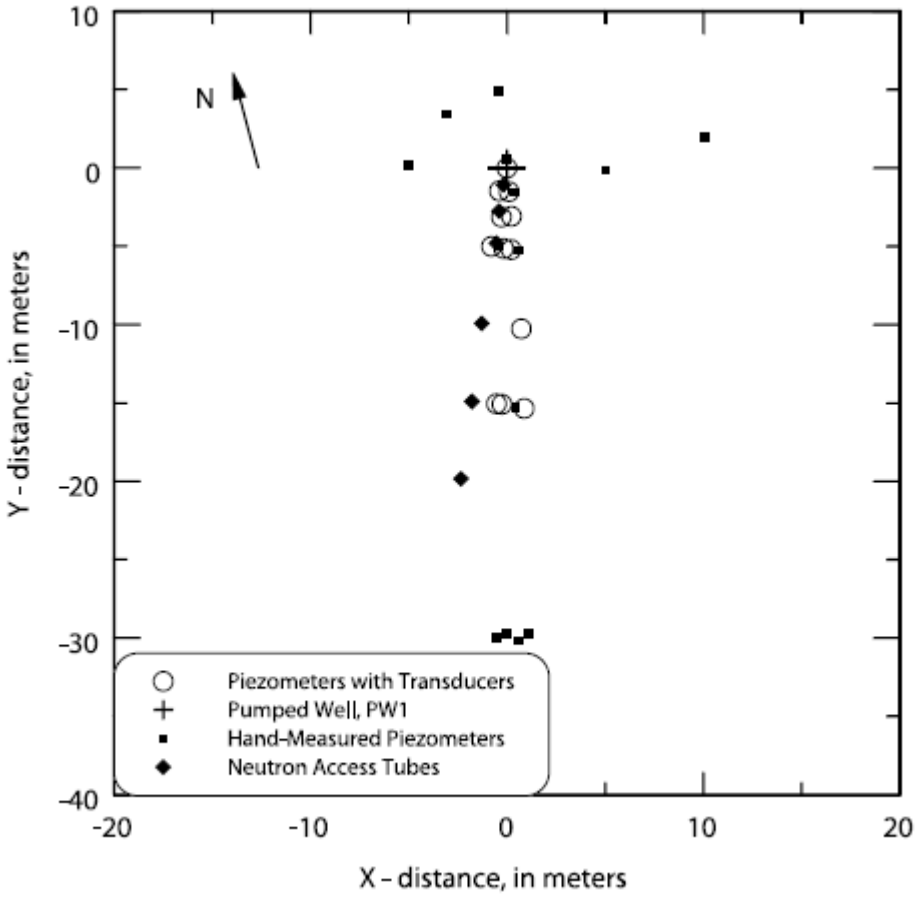


Figure 2: Plan view of the Borden test site showing the positions of the pumping well, the piezometers with transducers, the piezometers measured by hand, and the neutron access tubes. [*Moench*, 2008]

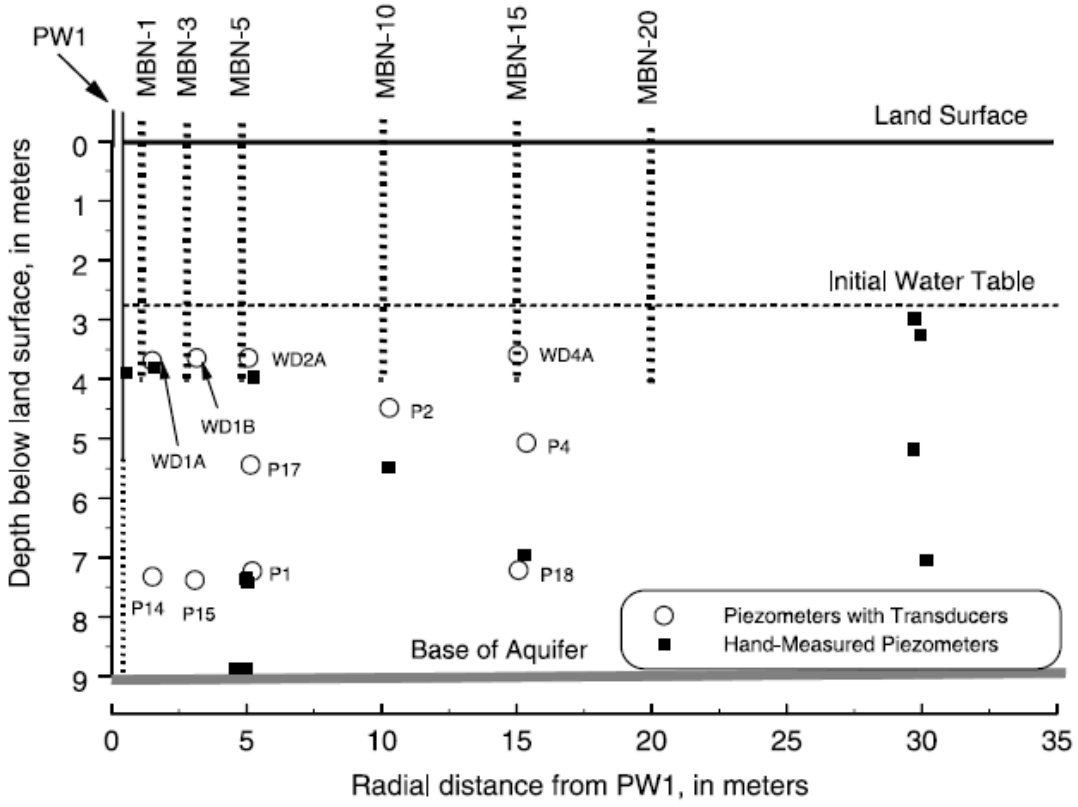


Figure 3: Vertical section of the aquifer at the Borden test site showing the position of the pumping well screen, the labeled piezometers with the transducers, the piezometers measured by hand, and the neutron access tubes. [*Moench*, 2008]

Table 1. Radial distance of the observation piezometers from pumping well and depth of the piezometers.

| Well Number | Radial Distance, m | Depth, m |
|---|---|---|
| WD1A | 1.51 | 0.94 |
| P14 | 1.51 | 4.57 |
| WD1B | 3.15 | 0.89 |
| P15 | 3.08 | 4.63 |
| WD2A | 5.07 | 0.89 |
| P17 | 5.15 | 2.69 |
| P1 | 5.22 | 4.48 |
| P2 | 10.28 | 1.73 |
| WD4A | 15.05 | 0.84 |
| P18 | 15.07 | 4.46 |
| P4 | 15.36 | 2.32 |

3.2 Analytical models

The analysis of the drawdowns is done with three analytical models: (1) Neuman Model (saturated zone only with instantaneous drainage onto the water table), (2) Moench model (saturated zone only with delayed drainage described by three empirical constants in the water table boundary condition), and (3) Mathias-Butler model (saturated zone coupled with unsaturated zone using richard's equation with exponential expressions for unsaturated hydraulic properties). Appendix A describes the analytical models in more detail. WTAQ4, a FORTRAN code developed by *Moench* [2008] to calculate drawdowns from the above three models is used in the analysis. The code allows for numerical inversion of Laplace transform by both *Stehfest* [1970] and *de Hoog et al.* [1982]. Included in the code are wellbore storage, wellbore skin effect, and delayed piezometer response. We have modified the WTAQ4 code by adding a subroutine to calculate velocity of the water table and velocity of drainage below the water table. The modified WTAQ4 code can be obtained at request from the author.

*Endres et al.* [2007] made a similar analysis using WTAQ which is an early version of WTAQ4, and a nonlinear parameter estimation algorithm PEST, to calculate the drawdown of the water table and storage in the unsaturated zone in an unconfined aquifer without considering wellbore skin effect and delayed piezometer response. Both *Moench* [2008] and *Endres et al.* [2007] performed the aquifer test analysis using WTAQ coupled with PEST. *Moench* [2008] considered data from the piezometers with transducers and hand measured drawdowns whereas *Endres et al.* [2007] used only pressure transducers measurements. *Endres et al.* [2007] did not include data after

360,000 s in the pumping test analysis because of the impact from a possible distant recharge boundary. The saturated zone hydraulic parameters remained consistently close for the different models analysed by *Moench* [2008] and *Endres et al.* [2007]. Table 2 describes the parameters derived from the pumping test analysis coupled with PEST obtained by *Moench* [2008] and *Endres et al.* [2007]. This study is done with the parameters derived by *Moench* [2008].

PEST algorithm determines parameter values that result in a minimization of squared differences between measured drawdowns in all wells and the drawdowns obtained by analytical models. In the Neuman and Moench models, which only deal with saturated zone in the aquifer test analysis, parameter estimation is done by calculating the least root mean square error (RMSE) between the measured drawdowns and the drawdowns from the models. Contrarily, the Mathias-Butler model is a more comprehensive one considering both saturated and unsaturated zones. Parameter estimation involves considering measured drawdowns in the saturated zone and soil moisture content in the unsaturated zone. The parameters from the Mathias-Butler model are obtained by fixing the moisture retention exponent ($a_c$ = 5 $min^{-1}$) and an adjustable relative hydraulic conductivity exponent ($a_k$). By assuming $a_c = a_k$ yields a value of $a_c$ = 0.228 $min^{-1}$, resulting in a moisture retention curve which deviates considerably from the measured data. Unless otherwise mentioned all the results in this study are obtained by using parameters from *Moench* [2008] for different models.

Table 2. Parameters obtained for different models by *Moench* [2008] and *Endres et al.*[2007].

| Parameters | Estimated value by *Endres et al.*[2007] | Estimated value by *Moench* [2008] |
|---|---|---|
| | **Neuman Model** | |
| $K_r$ (m/s) | 6.27E-05 | - |
| $K_z$ (m/s) | 2.79E-05 | - |
| $S_s$ ($m^{-1}$) | 5.78E-05 | - |
| $S_y$ | 0.201 | - |
| | **Mathias-Butler Model** | |
| $K_r$ (m/s) | - | 6.84E-05 |
| $K_z$ (m/s) | - | 2.90E-05 |
| $S_s$ ($m^{-1}$) | - | 3.76E-05 |
| $a_c$ ($m^{-1}$) | - | 5 |
| $a_k$ ($m^{-1}$) | - | 31.7 |
| $S_y$ | - | 0.25 |
| $S_w$ | - | 1.74 |
| | **Moench Model** | |
| $K_r$ (m/s) | 6.10E-05 | 6.70E-05 |
| $K_z$ (m/s) | 3.29E-05 | 3.05E-05 |
| $S_s$ ($m^{-1}$) | 7.19E-05 | 4.45E-05 |
| $S_y$ | 0.284 | 0.25 |
| $\alpha_1$ ($min^{-1}$) | 1.01E-02 | 4.42E-02 |
| $\alpha_2$ ($min^{-1}$) | 1.04E-02 | 6.90E-03 |
| $\alpha_3$ ($min^{-1}$) | 3.27E-04 | 1.65E-04 |
| $S_w$ | - | 1.66 |

Figure 4 shows the comparison of drawdowns obtained from the Moench model with the observed drawdowns. The piezometer delayed response; wellbore storage and skin effect are included in WTAQ4 to obtain the drawdowns using the Moench model. Not shown in the figure are the drawdowns from the Mathias-Butler model as the drawdowns are very close to the Moench model. The RMSE for the drawdowns from the Mathias-Butler and Moench models using the parameters in Table 2 are 0.0228 and 0.0248 m, respectively [*Moench*, 2008]. The drawdowns from the Moench model give a reasonable agreement with the field drawdowns, except for the shallow wells in the vicinity of the pumping well and the observation wells far from the pumping well. Deviation of drawdowns for observation wells far from the pumping well may be attributed to the fact that, there is possible interaction with a distant recharge boundary. Drawdowns from the Moench model overestimate the field drawdowns from observation piezometers of P1, P18, P2 and WD4A. Subsequently in this study, these drawdowns from different models are used to calculate the water table drawdowns, velocity of the free surface and velocity of drainage below the water table. Influence of the unsaturated zone was partially addressed in the Mathias-Butler model by assuming exponential soil hydraulic properties and only vertical flow in the unsaturated zone. The evidence of horizontal flow in the unsaturated zone, demonstrated by *Silliman et al.* [2002] and *Moench* [2008], demands the need for a better analytical solution considering vertical and horizontal flow in both saturated and unsaturated zones. *Mishra and Neuman* [2010, in press] improved the solution of *Tartakovsky and Neuman* [2007] by allowing a more flexible representation of the unsaturated zone including a finite thickness of the

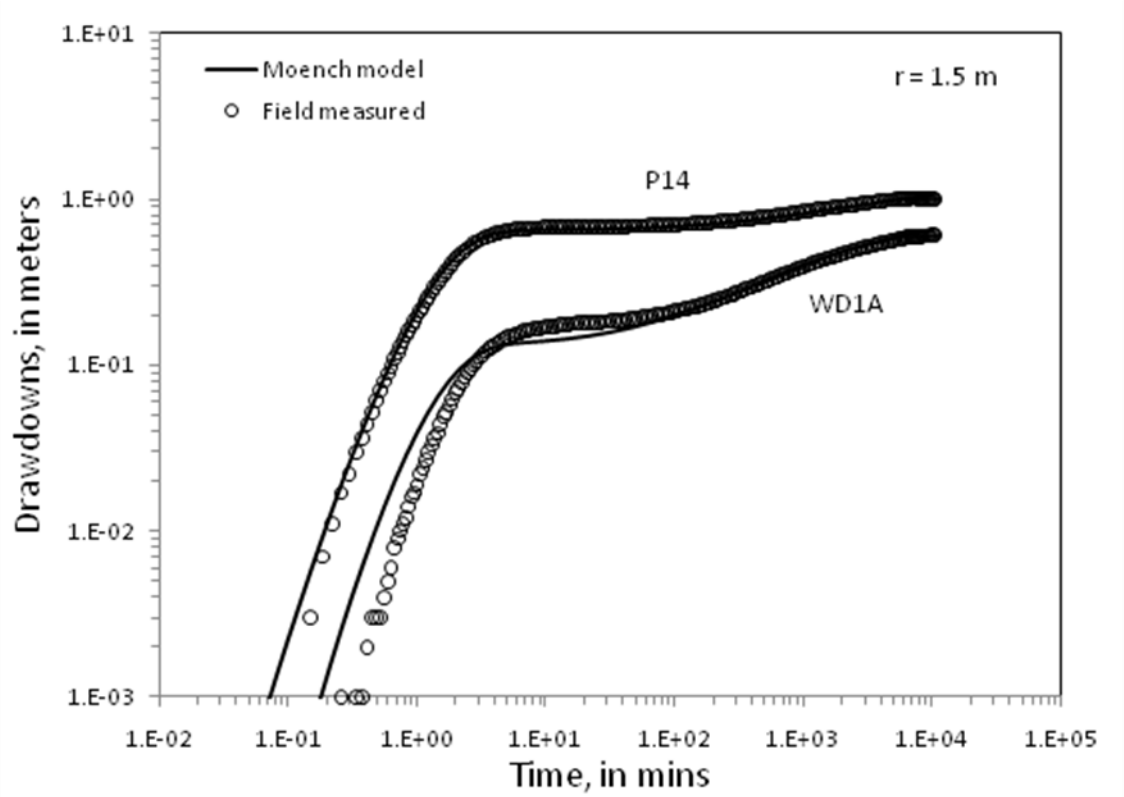


Figure 4: Comparison of measured drawdowns (circles) for piezometers as listed in Table 1 with analytical responses (solid) from Moench model including delayed piezometer response using the parameters in Table 2.

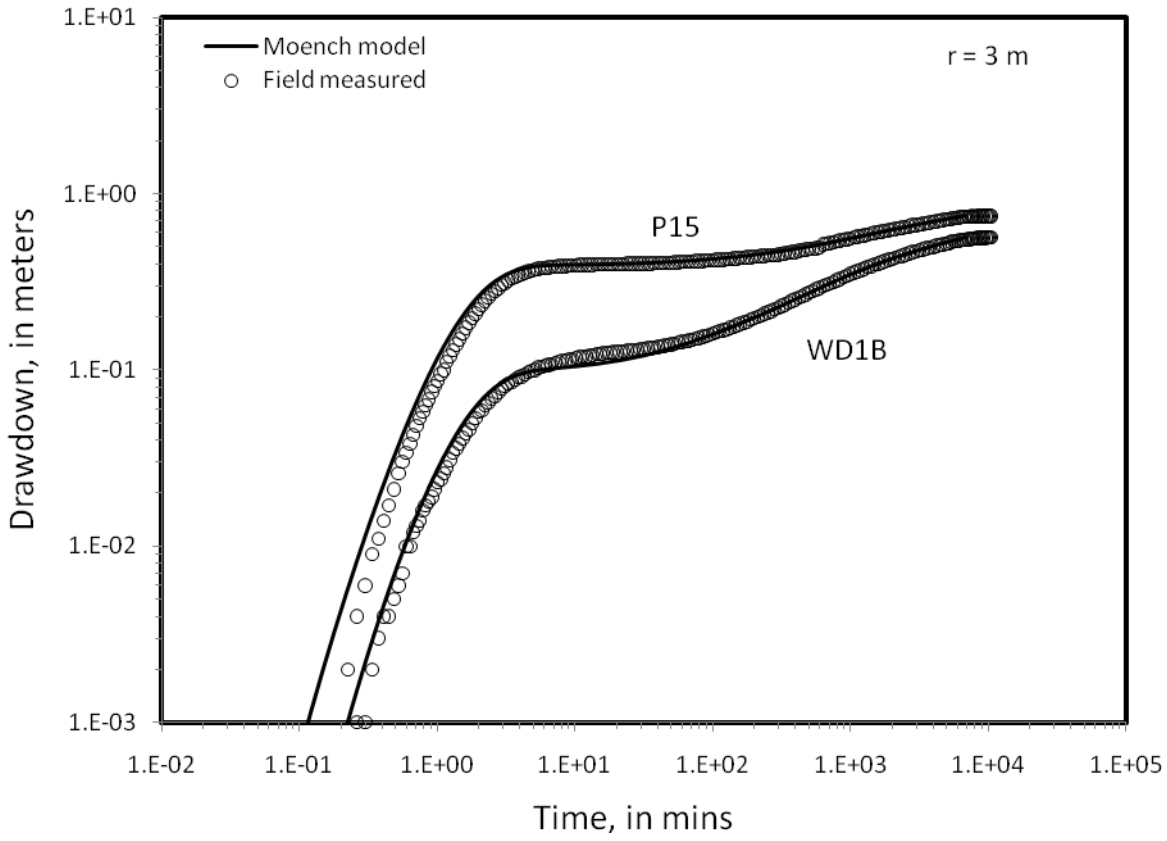


Figure 4: Continued.

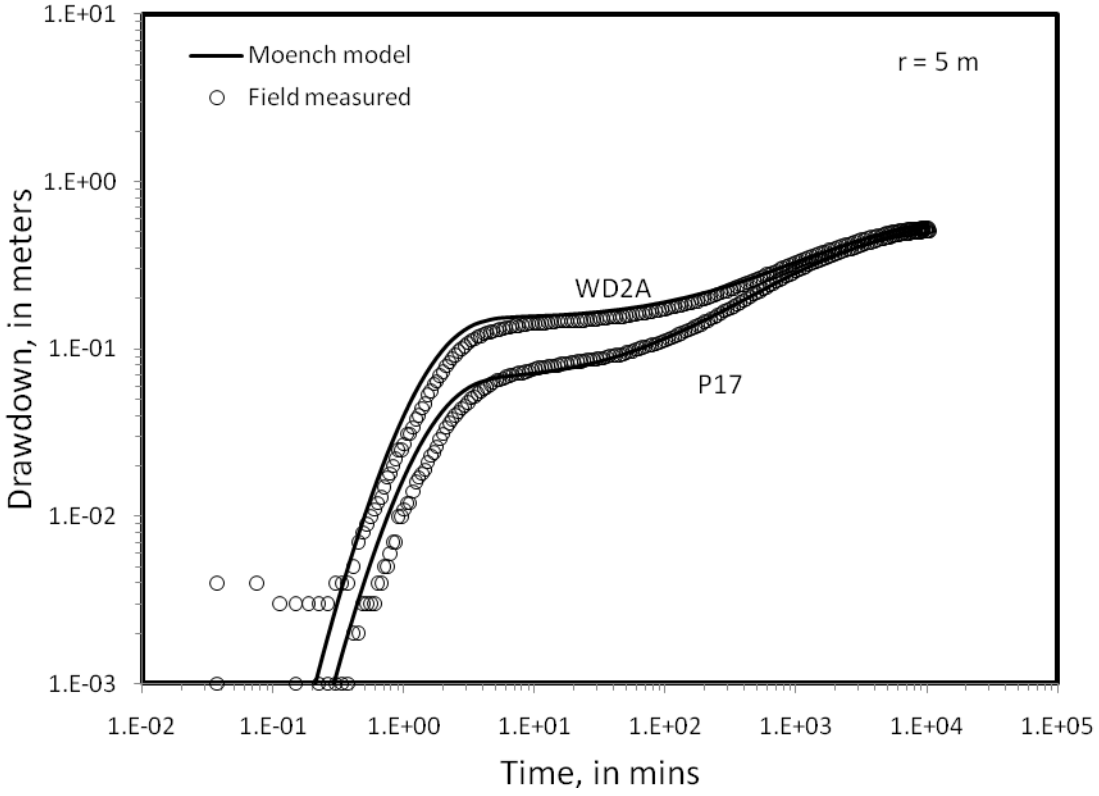


Figure 4: Continued.

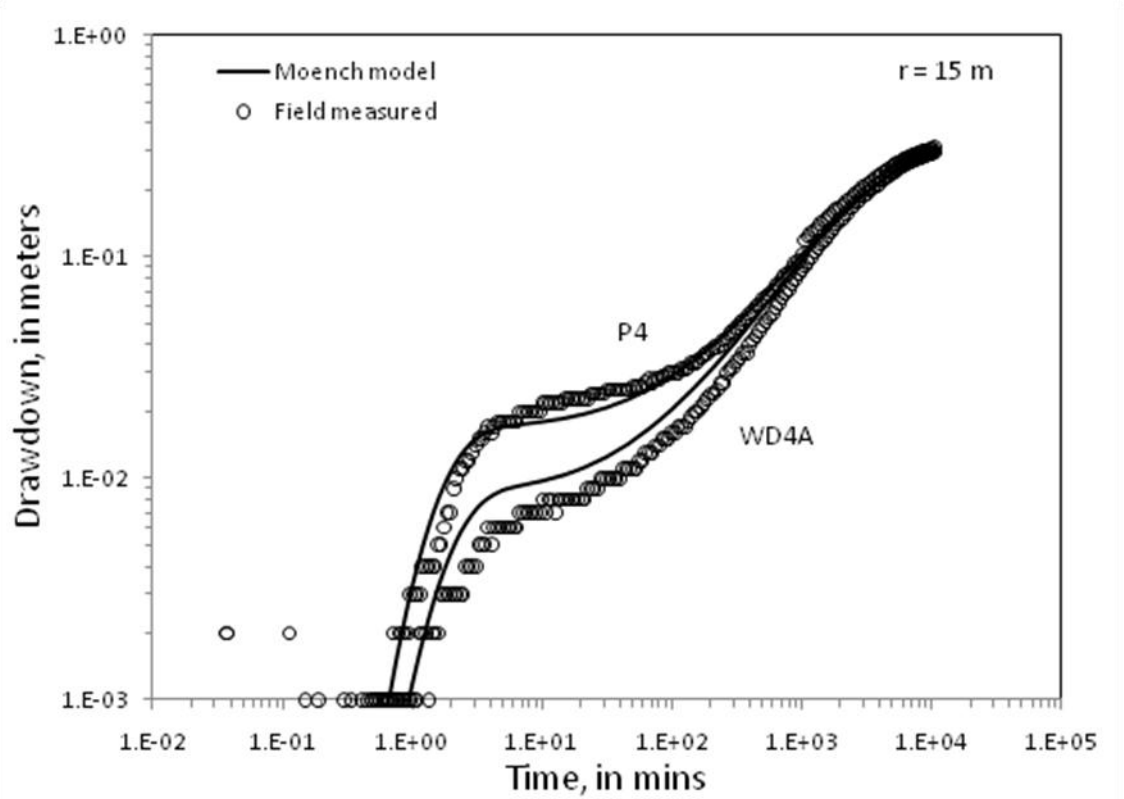


Figure 4: Continued.

unsaturated zone and horizontal flow in the unsaturated zone. *Mishra and Neuman* [2010, in press] solution is not included in this study, but the derived analytical solution can be used to obtain both the saturated and unsaturated zone properties. The numerical model, VS2DT 1.3, is used in the next section to consider both vertical and horizontal flow in the saturated and the unsaturated zones.

3.3 Numerical model

The USGS computer model, VS2DT [*Lappala et al*., 1987; *Healy*, 1990; *Hsieh et al.*, 2000] is a numerical code used in the current analysis. This 2-D axisymmetric finite-difference model can simulate fluid flow in variably saturated media by accepting parameters for both saturated and unsaturated zones. The governing equation is a 2-D equation in the *r*-*z* domain, in which *r* is the radial direction and *z* is the vertical direction.

A graphical user interface developed by *Hsieh et al.* [2000] is used to define the model. The unsaturated zone is represented by the soil hydraulic characteristic functions of Brooks and Corey model.

For $h < h_b$,

$$S_e = \left( \frac{h}{h_b} \right)^{-\lambda}, \tag{1}$$

$$k_r = \left( \frac{h}{h_b} \right)^{-2-3\lambda} . \tag{2}$$

For $h \geq h_b$,

$$S_e = 1, k_r = 1, \tag{3}$$

where $S_e = (\theta - \theta_r)/(n - \theta_r)$ is effective saturation, $\theta$ is volumetric moisture content, $\theta_r$ is residual moisture content, $n$ is porosity, $k_r$ is relative hydraulic conductivity, $h$ is pressure head, $h_b$ is bubbling or air entry pressure head, $\lambda$ is pore-size distribution index.

All the parameters are the same as the fitting parameters obtained by *Moench* [2008] by running parameter estimation algorithm PEST with VS2DT. The $\lambda$ value of 0.435, obtained by *Moench* [2008], resulted in an unrealistically rapid drop in soil volumetric moisture content. *Moench* [2008] made an additional run by forcing $\lambda$ to match the soil moisture observations resulting in a $\lambda$ value of 2.5. We want to emphasize that it is important to use appropriate value for $\lambda$ for realistic unsaturated zone characterization. Drawdowns obtained using VS2DT are shown in Figure 5 wherein $\lambda$=2.5. With the increase of $\lambda$ from 0.435 to 2.5, the RMSE obtained from the drawdowns in the saturated zone increased from 0.0246 m to 0.0337 m, resulting in a degradation of the match between measured and simulated drawdowns.

The VS2DT model is set up with the initial equilibrium profile by defining the height of the water table and the height of the minimum pressure head. The minimum pressure head is the negative of the height above the water table when the saturation equals the residual water saturation. The total head below the minimum pressure head elevation is uniform in the domain; and the pressure above the minimum pressure head elevation is equal to the minimum pressure head. The parameters defined for the aquifer, well skin and the pumping well are shown in Table 3. The grid extends from very fine columns, near the pumping well and the observation piezometers, to coarse columns distant from the pumping well. Similarly the rows are very fine, near the water table and

Table 3. Parameters used to run VS2DT with Brooks and Corey model.

| **Parameter** | **Aquifer** | **Pumping well** | **Well skin** |
|---|---|---|---|
| porosity | 0.37 | 1 | 0.37 |
| Residual moisture content | 0.07 | - | 0 |
| saturated $K_r$ (m/s) | 6.60E-05 | 10 | 1.80E-05 |
| $K_z/K_r$ (m/s) | 0.5 | 1000 | 1 |
| specific storage | 3.50E-05 | 1 | 3.50E-05 |
| $\lambda$ | 2.5 | - | - |

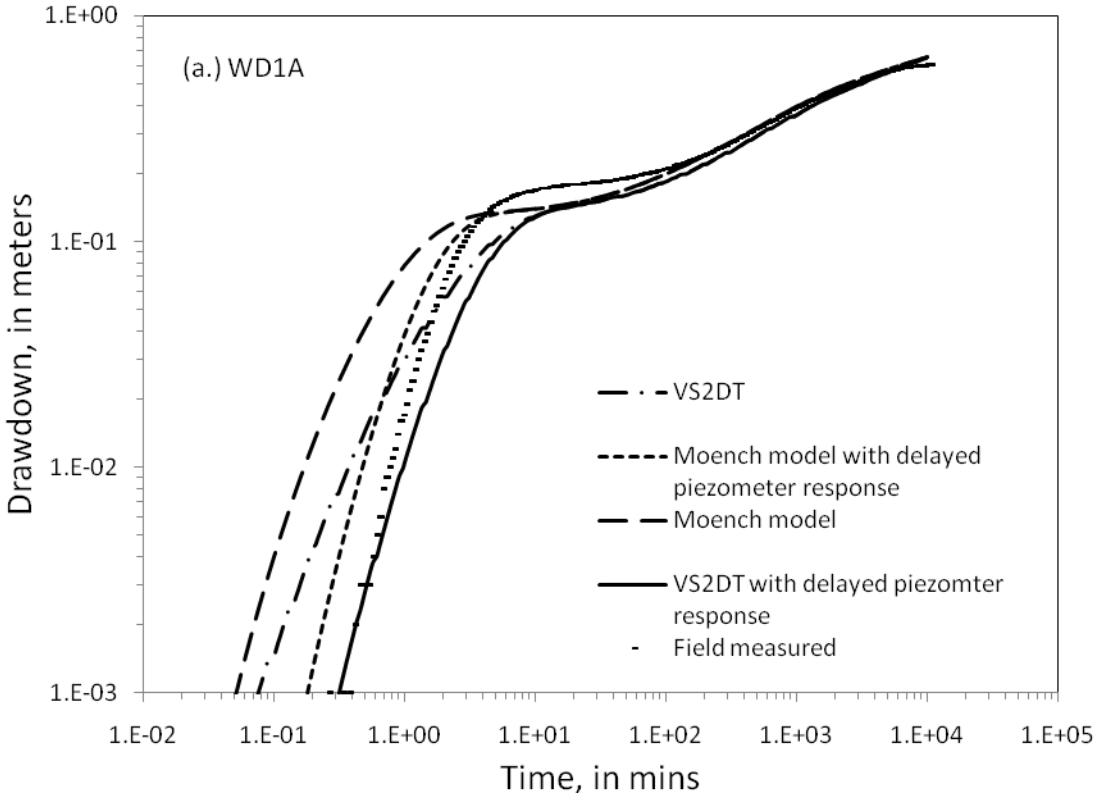


Figure 5: Comparison of measured drawdowns for piezometers as listed in Table 1 with drawdowns obtained from VS2DT and the Moench model with and without delayed piezometer response using the parameters in Table 2.

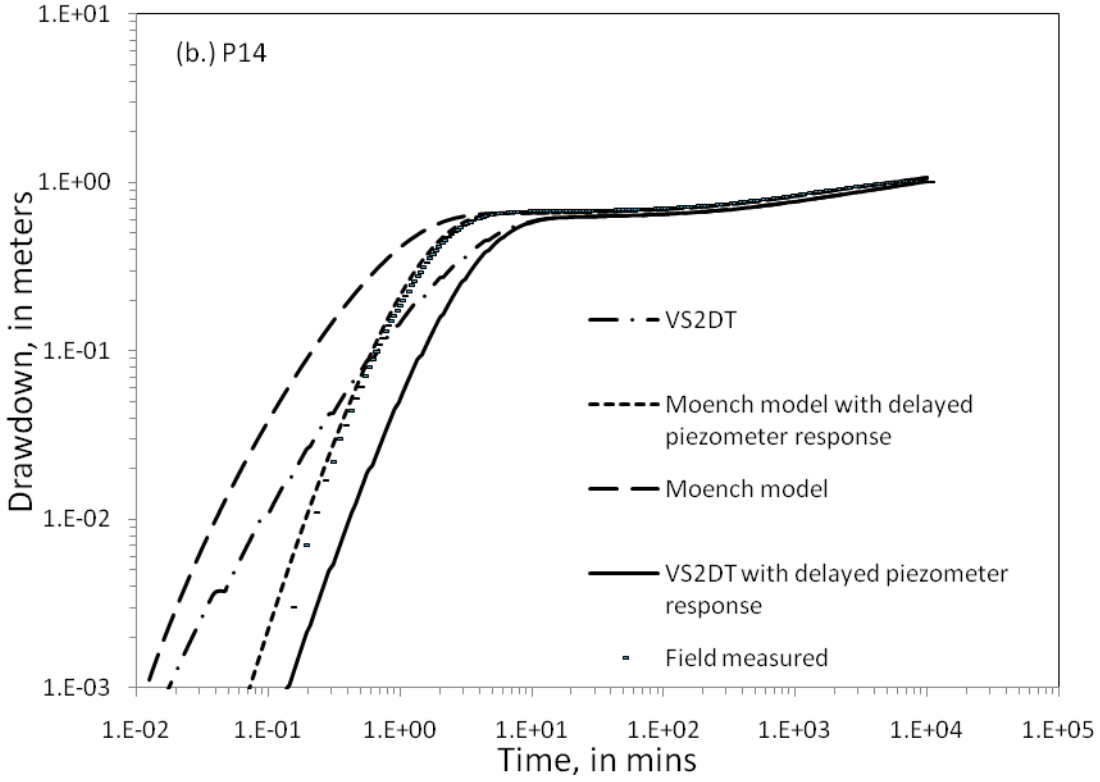


Figure 5: Continued.

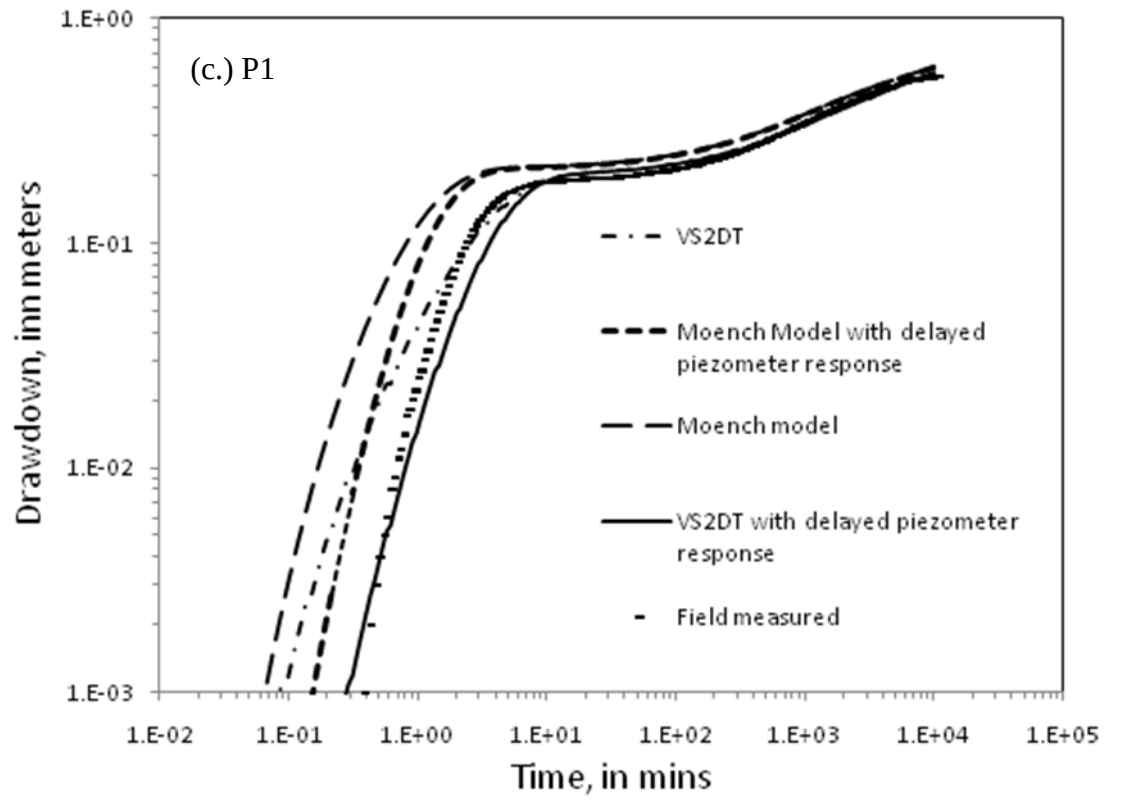


Figure 5: Continued.

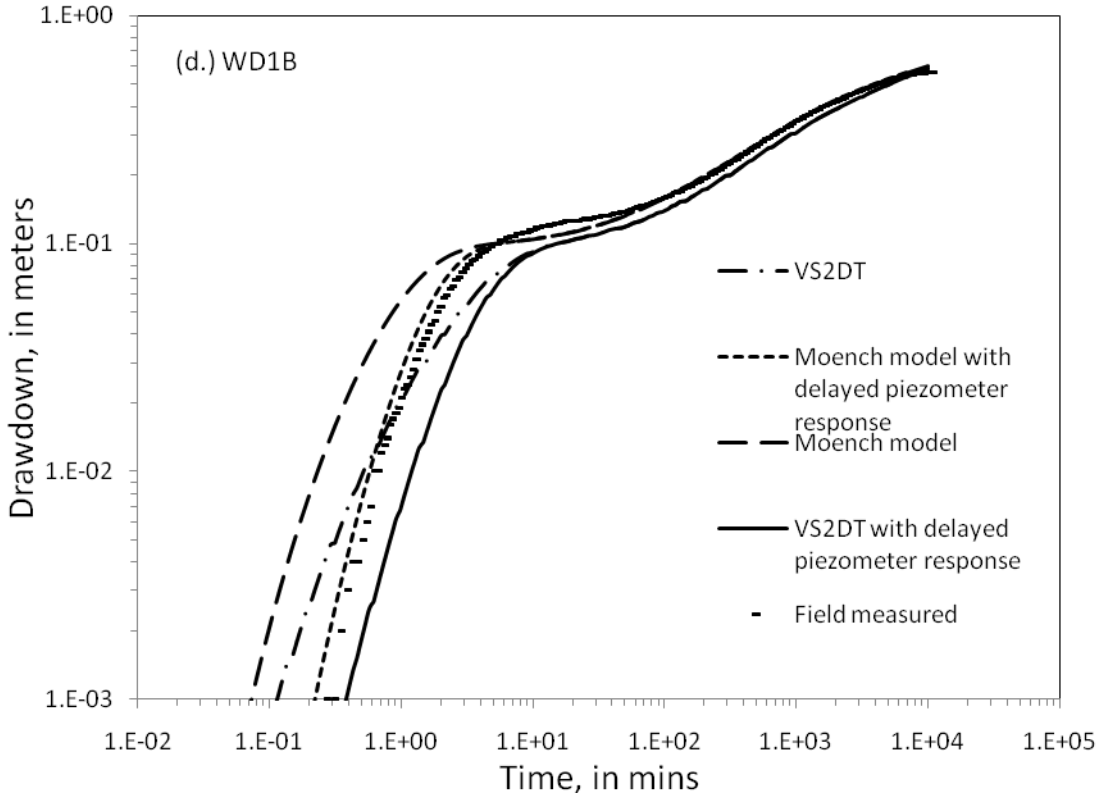


Figure 5: Continued.

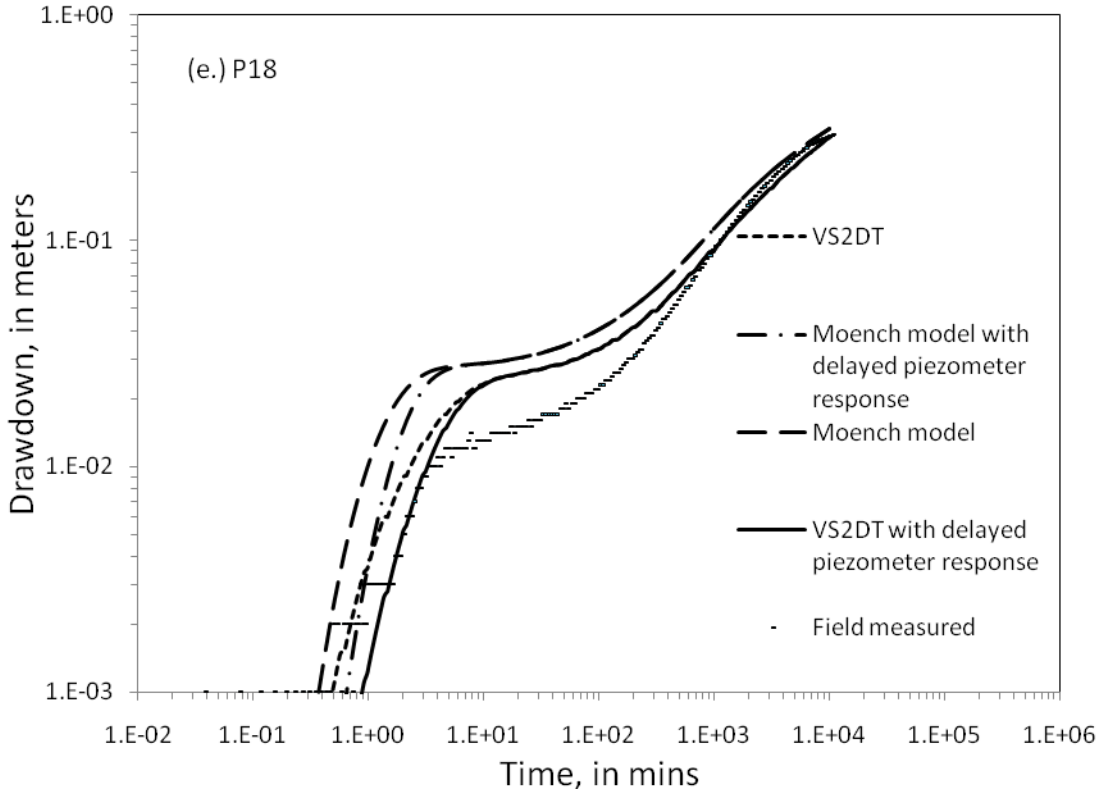


Figure 5: Continued.

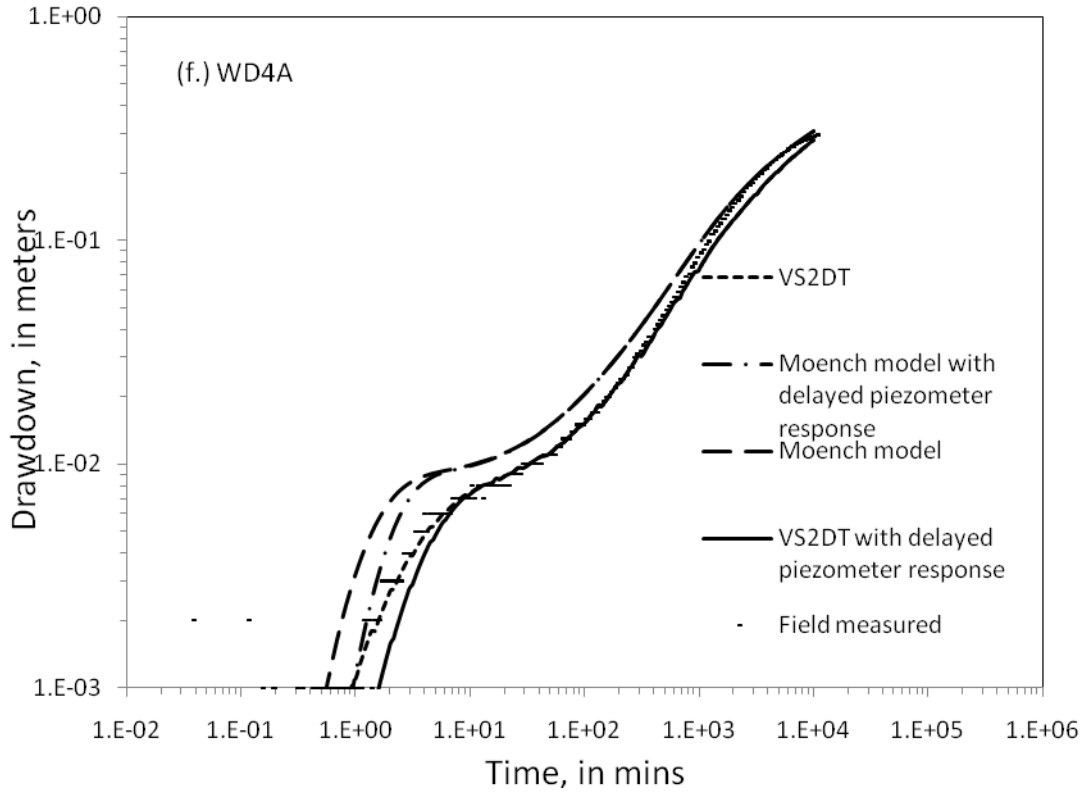


Figure 5: Continued.

the observation piezometers, and coarser near the bottom boundary. Screened over the bottom 3.75 m, the pumping well is defined as a zone with high hydraulic conductivity and porosity equal to 1. The pumping rate is equal to 6.67E-04 $m^3$/sec and is defined as a volumetric flow rate boundary condition at 0.6 m above the top of the screen (A. Moench, written communication, February 2010). The hydraulic conductivity in the well bore was assumed essentially. By using the analytically derived hydraulic conductivity of the aquifer and the above mentioned parameters for the pumping well, the hydraulic conductivity of the skin is adjusted to get the best fit between the measured and simulated drawdowns in the pumping well.

Figure 5 a-f shows the log-log plot of the comparison between the field drawdowns and drawdowns obtained from the VS2DT model with and without piezometer delayed response. The drawdowns from Moench model with and without piezometer delayed response are included in the figure for reference. The WTAQ4 numerical code provides the user with the option to calculate drawdowns with or without piezometer delayed response. The drawdowns from the analytical models are corrected for delayed response by *Moench* [1997] using the differential equation derived by *Hvorslev* [1951].

$$\pi r_p^2 \frac{dh_m}{dt} + \frac{FK_r h_m}{2\pi} = \frac{FK_r h}{2\pi}, \qquad (4)$$

where $r_p$ is the radius of the piezometer, $h_m$ is the measured hydraulic head, $K_r$ is the saturated radial hydraulic conductivity, and $F$ is the shape factor defined by *Hvorslev* [1951] as $F = \frac{L}{\ln(k + (1+k^2)^{0.5})}$, $k = \left(\frac{K_r}{K_z}\right)^{0.5} \frac{L}{2r_p}$, where $L$ is the screen length of the piezometer and $K_z$ is the saturated vertical hydraulic conductivity.

It is evident from Figure 5 that, in most of the piezometers the deviation of the simulated drawdowns from the field drawdowns is much larger at the early and intermediate time without considering the delayed response. Although the late time drawdowns are reliable to calculate the specific yield, the specific storage depends on the rapidly changing early time drawdowns. The formulation derived by *El-Kadi* [2005] for delayed response is used to correct the drawdowns at monitoring wells obtained by VS2DT. *El-Kadi* [2005] expanded the solution to consider delayed response based on the previous work of *Hvorslev* [1951] and *Moench* [2008].

Eq. (4) is rearranged and integrated to obtain:

$$\frac{h_m}{h} = \left[1 - \exp(-at)\right], \qquad (5)$$

where $a = (FK_r)/(\pi r_p^2)$.

The addition of delayed response factor for monitoring wells greatly improved the fit between the measured and simulated drawdowns at the early time but the late time results remained relatively unaltered. Figure 5 shows the match between measured and simulated drawdowns obtained from VS2DT after including delayed response. Drawdowns derived from VS2DT in piezometers WD1A, P1, P18 and WD4A gave a better fit than drawdowns from the Moench model. In all the other transducer measured piezometers, the Moench model resulted in a better fit between measured and simulated drawdowns. This indicates that VS2DT predicts accurate drawdowns in the piezometers far from the pumping well and at shallow depths from the water table compared to the Moench model which represents the drawdowns better in the deep seated piezometers.

### 3.4 Water table drawdown analysis

All derived results in this study, including water table drawdown, velocity of water table, and velocity of drainage, are calculated from the hydraulic head values. The predicted location of the specific potentiometric surface at different times is essential to calculate velocity of the water table. Further, in this study the specific potentiometric surface is used to represent water table defined as the surface with pore pressure at atmospheric pressure. We included the process of calculating water table drawdowns in the newly added module to WATQ4. Tracking of the water table is done by calculating drawdowns at a set of points below the initial water table. When the drawdown at a point equals the depth of that point below the initial water table, the pressure head at that time is zero or the total head becomes the elevation from the datum.

The vertical head gradient is assumed to be constant when calculating the water table time-drawdowns. This assumption will be tested in later discussion. A similar process is followed in VS2DT to calculate the water table time-drawdown by manually placing hypothetical observation wells at depth intervals of 1 cm below the water table. As shown in Figure 6, the starting time for the water table time-drawdown obtained from VS2DT is when the water table drawdown is 1 cm.

The field water table drawdown at a given radial distance is obtained by extrapolating the drawdowns from the vertically displaced piezometers. To obtain the water table drawdown as mentioned above, the vertical gradient of drawdown is also assumed to be constant. To verify the assumption that drawdowns vary linearly with depth, the pressure head profile along transects at 1.47 m and 3 m obtained from the

Moench model are plotted in Figure 7. The pressure heads vary linearly with depth at different radial distances at both the early and late times, affirming the assumption of linear variation of drawdowns over depth. Although the pressure head varies linearly with depth, the vertical gradient of pressure head changes with both time and radial distance. The water table drawdown $\Delta h_{wt}$ can be estimated as [*Endres et al.*, 2000]:

$$\Delta h_{wt} = (\Delta h^u - m d^u)/(1-m), \quad (6)$$

where $\Delta h^u$ is the drawdown in an upper observation well and $d^u$ is the depth below the initial water table to the screen of the upper well, and *m* is the vertical hydraulic gradient given by

$$m = (\Delta h^l - \Delta h^u)/\Delta l, \quad (7)$$

where $\Delta h^l$ is the drawdown in a lower observation well and $\Delta l$ is the vertical separation between the screened intervals of the upper and lower well pair.

Figure 6 describes the water table time-drawdowns from the field and from three analytical models at different radial distances. The Neuman model assuming instantaneous drainage clearly underestimates the water table drawdown compared to field drawdowns. The Moench model which assumes delayed drainage fits the field water table drawdowns much better than the Neuman model.

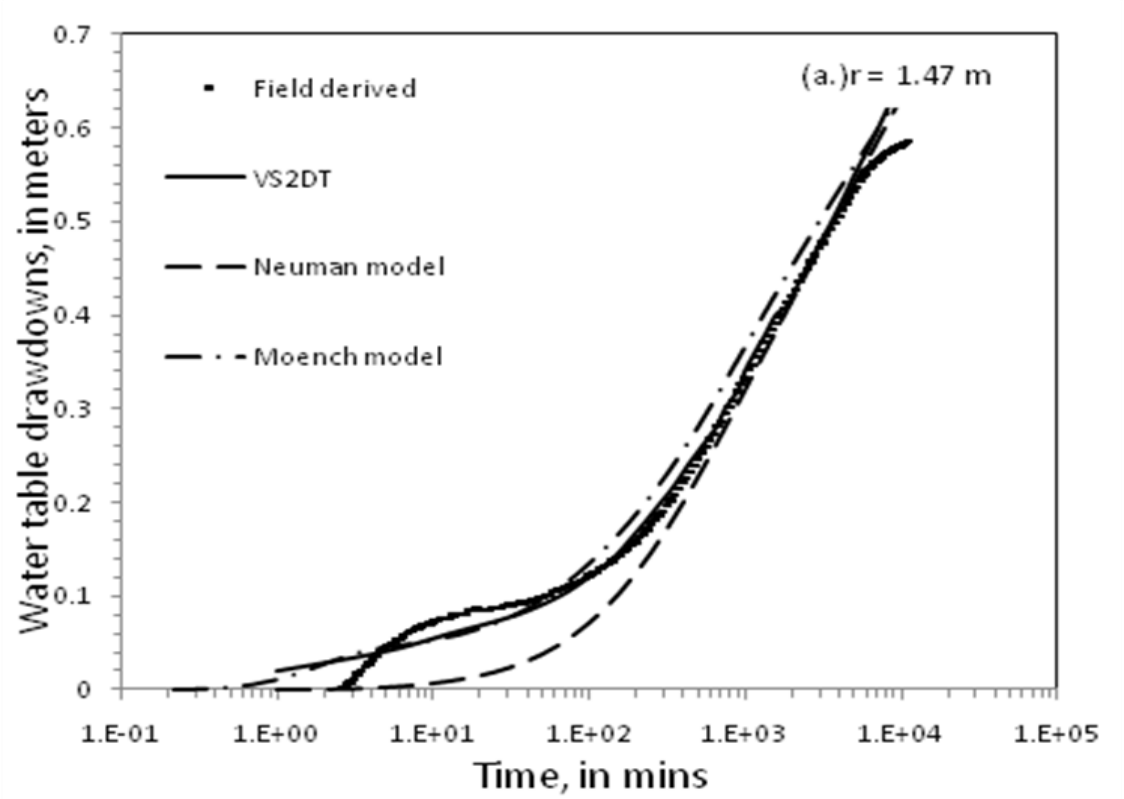


Figure 6: Comparison of measured water table drawdowns at radial distances of 1.47 m, 3 m, 5 m and 15 m with water table drawdowns obtained from the Neuman model, the Moench model (parameters in Table 2) and VS2DT (parameters in Table 3).

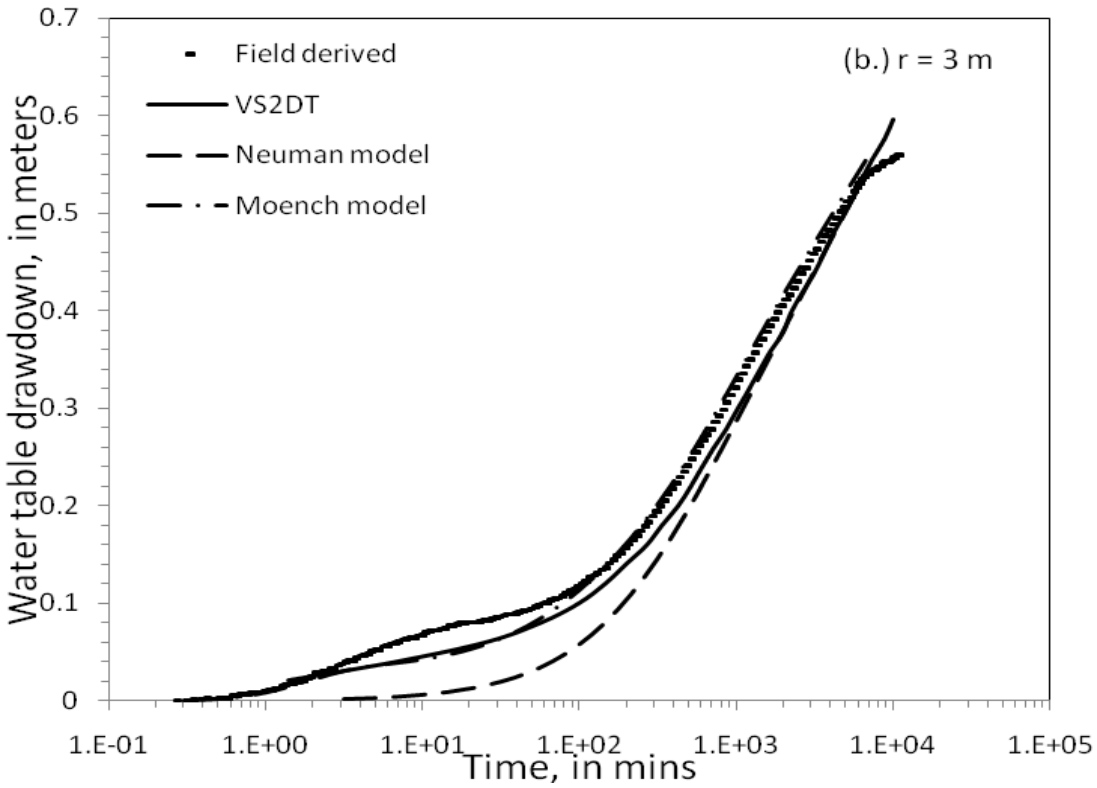


Figure 6: Continued.

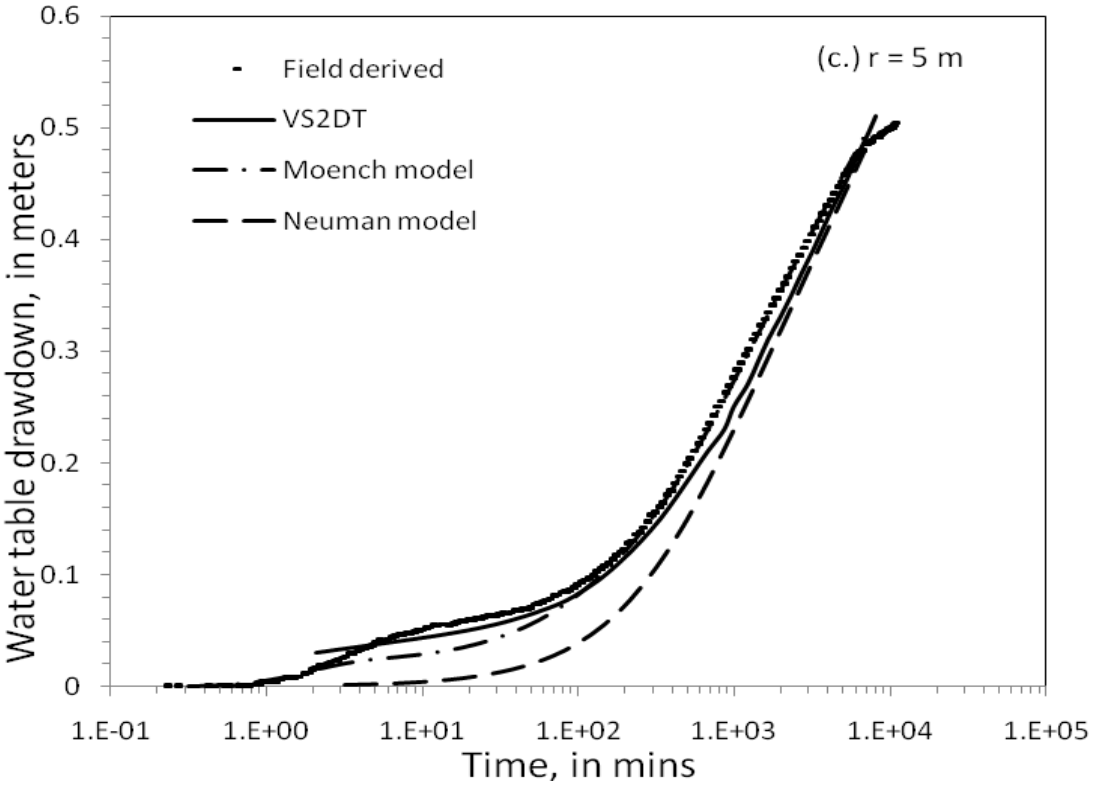


Figure 6: Continued.

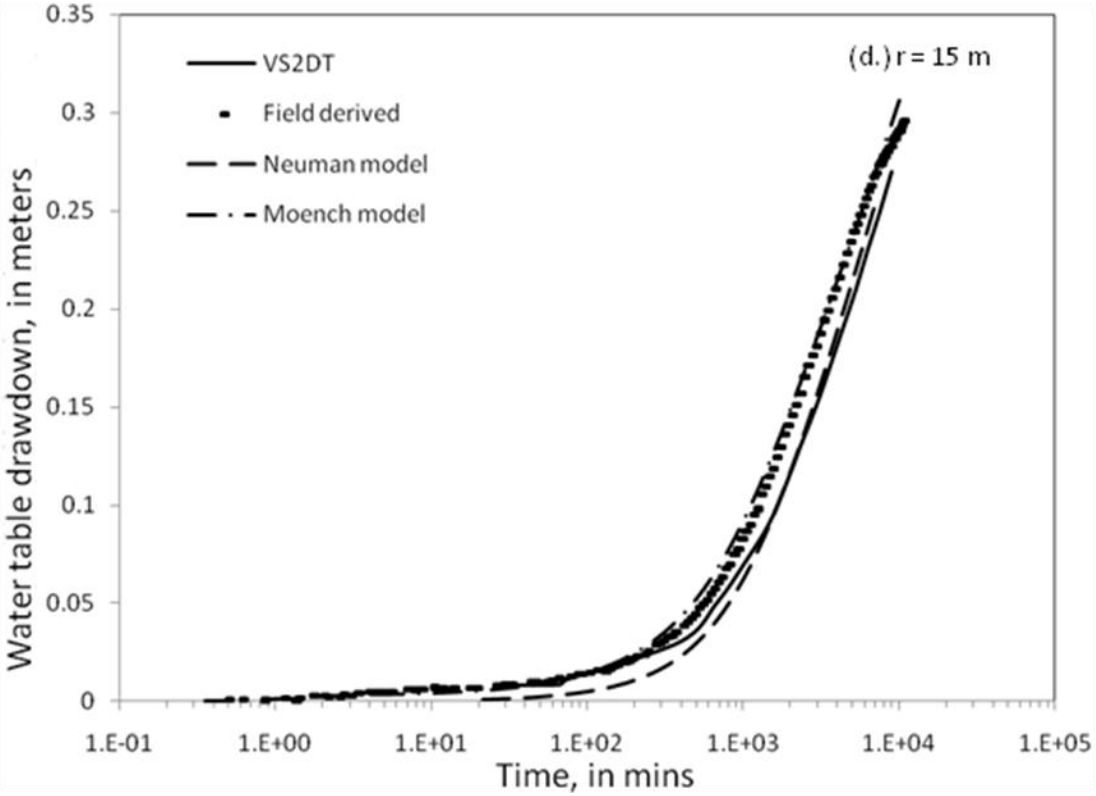


Figure 6: Continued.

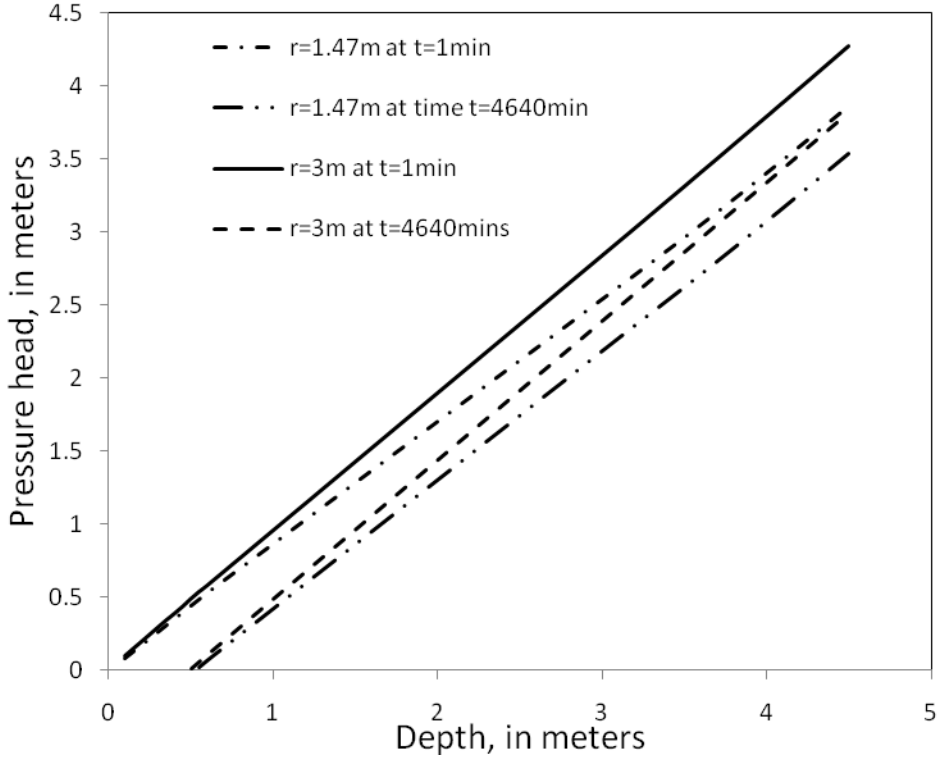


Figure 7: Variation of pressure head with depth, obtained from the Moench model at 1.47 m and 3 m at 1 and 4,640 mins.

# 4. VELOCITY ANALYSIS

## 4.1 Water table velocity estimation

Velocity of the water table is calculated based on the water table drawdown values. The water table drawdowns are obtained as discussed earlier in section 3. Both the water table drawdowns and velocity of the water table are determined by tracking the time taken for the water table to reach a designated depth. Velocity of the water table is the ratio of a small depth interval over the time taken for the water table to travel that interval. Such a depth interval varies between 1 mm to 1 cm. Such calculation of water table velocity has been employed in the numerical model VS2DT and the analytical models using WTAQ4. Velocity of the water table obtained from WTAQ4 remained relatively unaltered as the depth interval varies from 1 mm to 1 cm. Therefore, the depth interval of 1 cm is used in VS2DT. Velocity of water table is obtained as:

$$WTvel = (z_i - z_{i-1}) / (t_i - t_{i-1}), \quad (8)$$

where *WTvel* is velocity of the water table, $z_i$ is the depth of the water table at time $t_i$ and $z_{i-1}$ is the depth of the water table at time $t_{i-1}$. The depth interval of ( $z_i$ - $z_{i-1}$) is between 1 mm to 1 cm.

Figure 8 shows the semi-log plot for a typical water table velocity profile obtained from three analytical models. All three analytical models result in different peak velocities during the early time and converge to the same values at the late time. Figure 8 suggests that the water table moves slow initially to reach a peak velocity and then it decreases. This may be attributed to the increase in drainage from the unsaturated

zone to the water table. Figure 9 compares the water table velocity obtained from the analytical models with the field water table velocity. The peak velocity is not shown in measured values because of unreliable data in the first few. All three analytical models underestimate the water table velocity at 1.47 m as shown in Figure 9a. However, the Moench model results in a reasonable fit with the field water table velocities at 3 m and 5 m as observed in Figures 9b and 9c, respectively. *Endres et al.* [2007], in their study on bulk vadose zone response, observed that all three analytical models overestimated the cumulative drainage flux to the water table. Both the underestimation of water table drawdown and velocity of the water table at the early time can be due to overestimation of drainage by all three analytical models.

Figure 9 also shows the water table velocities obtained from VS2DT compared with field water table velocities. The calculation of water table velocity from VS2DT is obtained in a similar manner as for analytical models. The VS2DT model underestimates the water table velocity during the first few minutes; then it overestimates the water table velocity during the later time. Though the results obtained from VS2DT and the Mathias-Butler model does not overlap exactly, they follow the same trend of overestimating at the early time and underestimating at the late time. Both VS2DT and the Mathias-Butler model have considered integrated saturated-unsaturated flow processes. Further investigation on unsaturated parameter $\lambda$ used in VS2DT and $a_c$, $a_k$ used in the Mathias-Butler model may result in an overlap of findings obtained from VS2DT and the Mathias-Butler model.

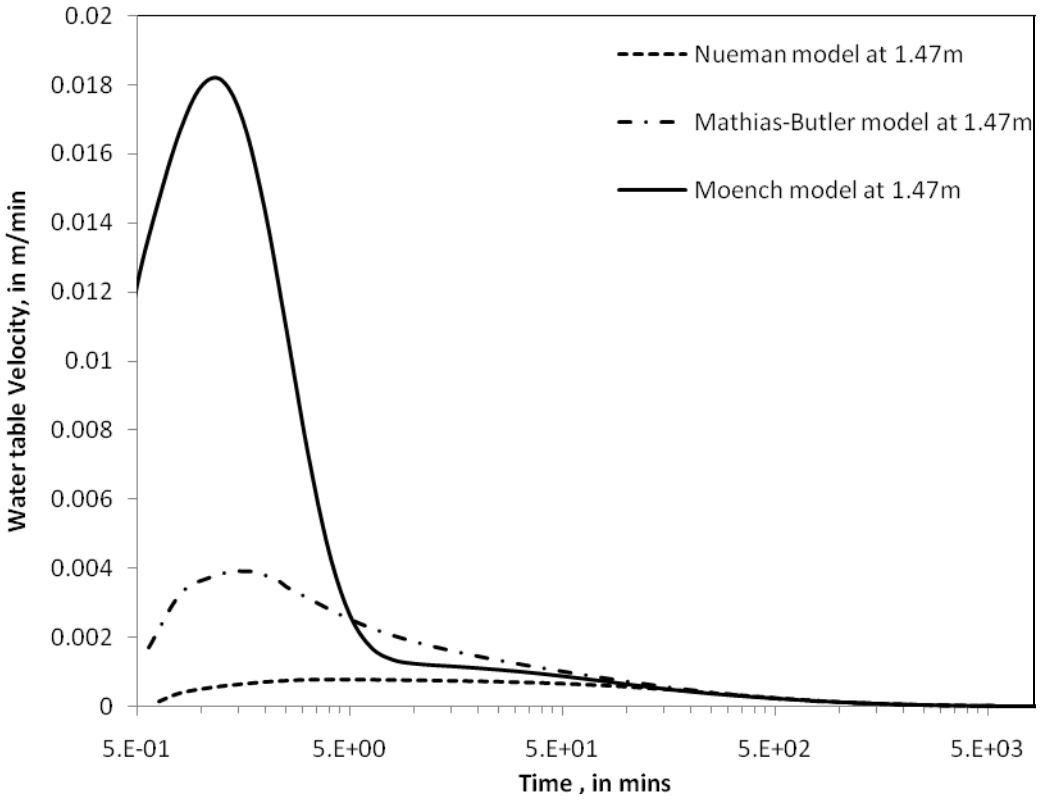


Figure 8: Typical water table velocity profiles obtained from the Neuman model, the Mathias-Butler model and the Moench model at radial distance of 1.47 m.

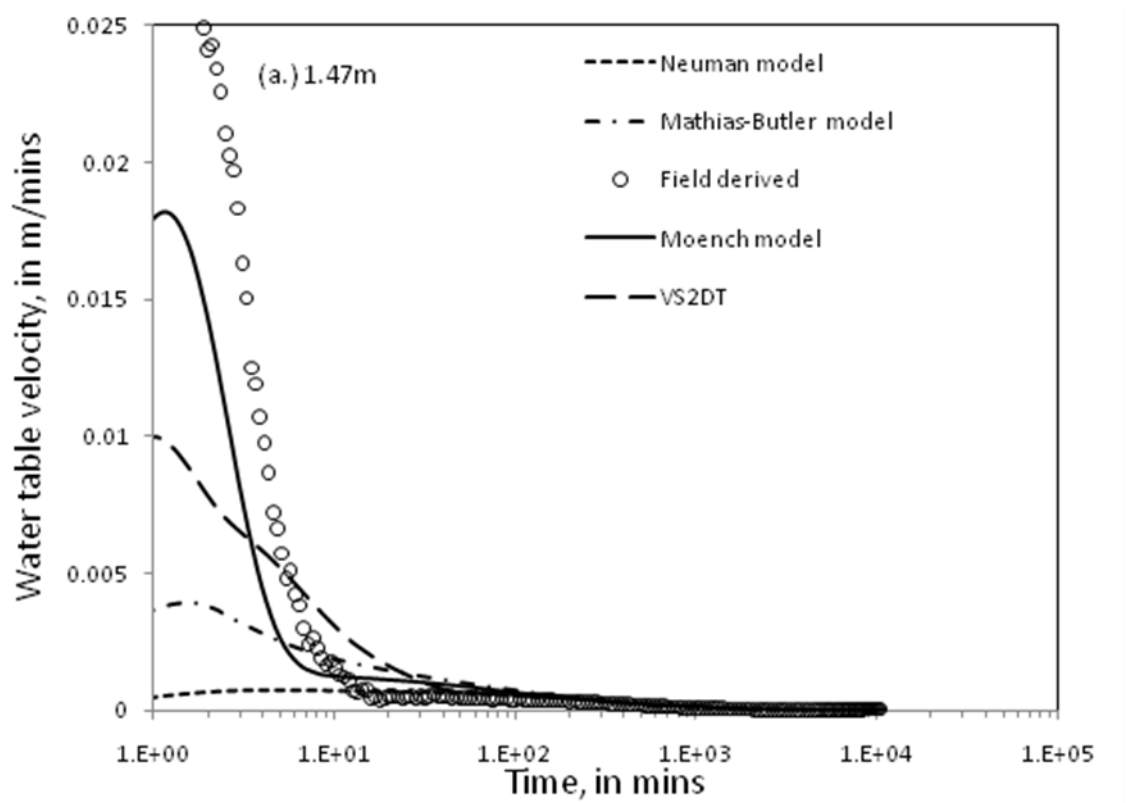


Figure 9: Comparison of measured water table velocities at radial distances of 1.47 m, 3 m and 5 m with water table velocities obtained from the Neuman model, the Moench model, the Mathias-Butler model and VS2DT using parameters in Table 2 and Table 3.

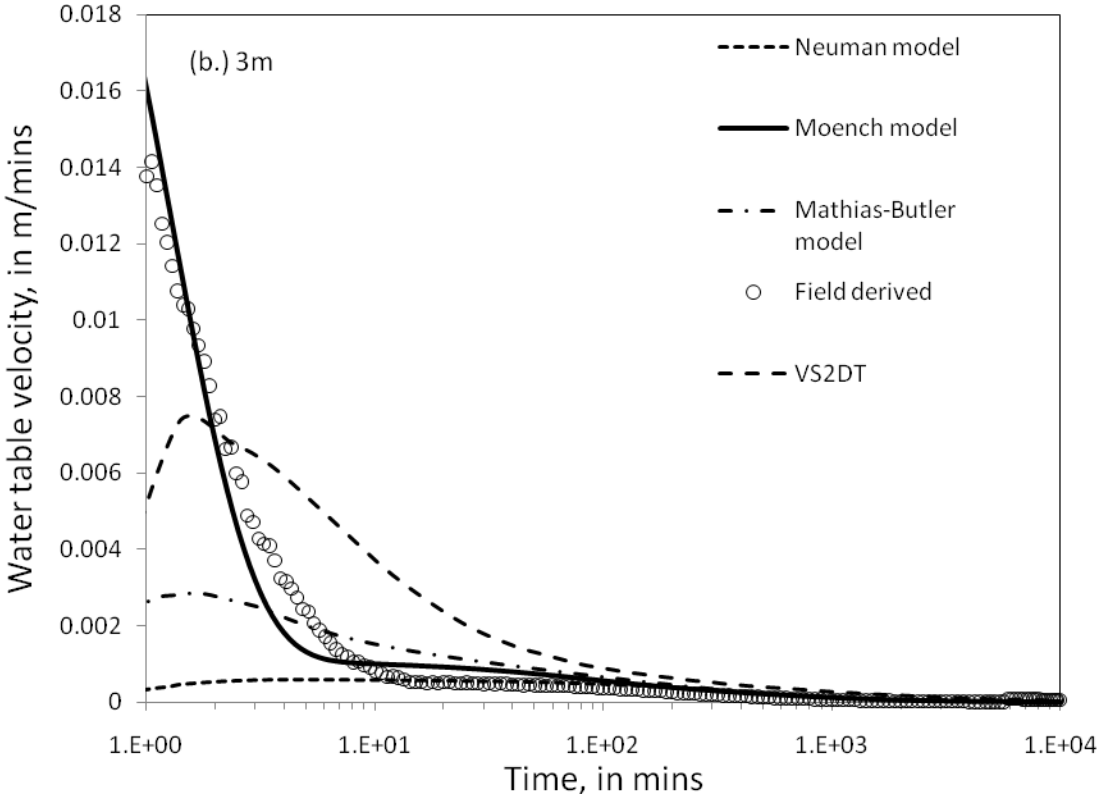


Figure 9: Continued.

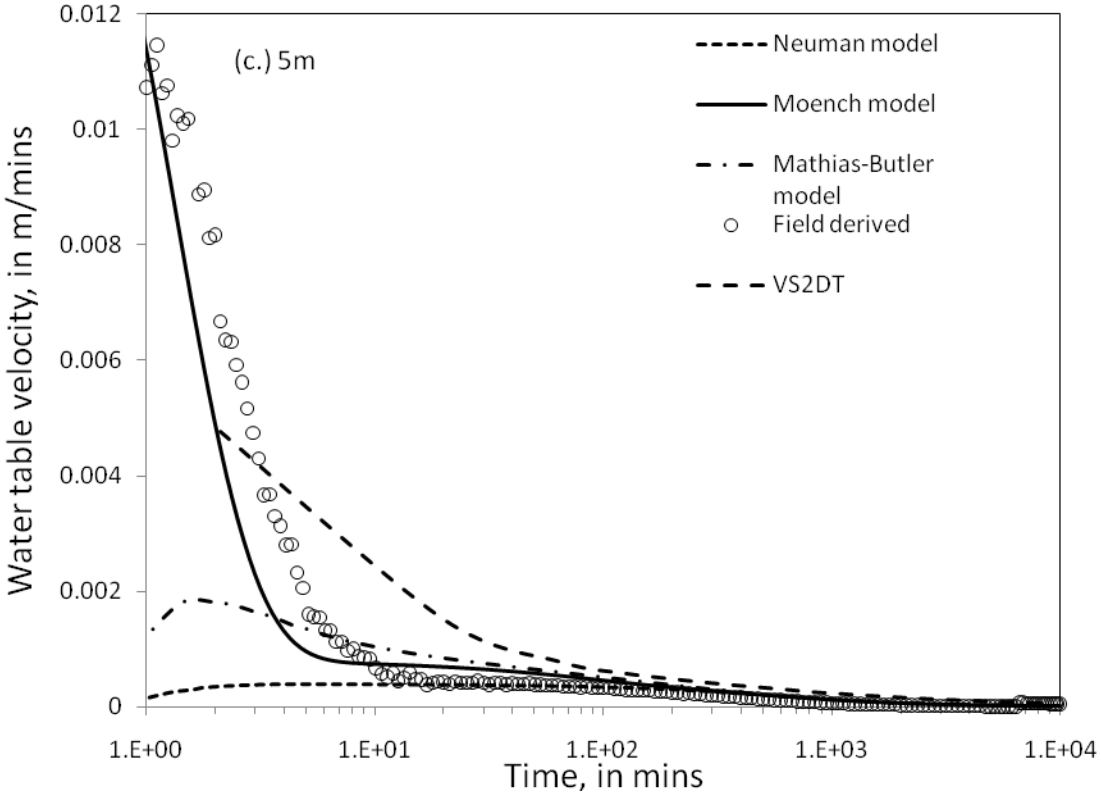


Figure 9: Continued.

4.2 Drainage velocity estimation

As described earlier, drainage velocity is the Darcy velocity of the water particles on the water table. Although the water particles on the water table experience both horizontal and vertical velocities, the vertical velocity determines the vertical motion of a material surface. The significance of including horizontal gradient in the boundary condition is discussed later. The drainage velocity is calculated as:

$$Drainage\ velocity = (K_z / S_y)\left(\frac{H_{z^*} - H_{z_i}}{z^* - z_i}\right), \qquad (9)$$

where $S_y$ is the specific yield, $z_i$ is the depth to the water table where the total hydraulic head is $H_{z_i}$, and $z^*$ is the depth slightly below the water table where the total head is $H_{z^*}$. The depth interval ($z_i$ - $z^*$) is sufficiently small (between 1 mm to 1 cm) to ensure that the head gradient is linear.

Figure 10 shows the drainage velocities obtained from VS2DT and three analytical models at different radial distances. The Neuman model predicts higher drainage velocity compared to other two analytical models due to the assumption of instantaneous drainage. The drainage velocities from the field cannot be calculated due to the absence of piezometers at sufficient depths below the water table. The average vertical groundwater velocities between the shallow and the deep seated piezometers are calculated from the Moench model and VS2DT, and are compared with their counterpart from the field, as shown in Figure 11. The Moench model overestimates the average vertical velocity and VS2DT slightly underestimates the average vertical velocity compared to the field values. The average vertical velocity obtained from the vertical

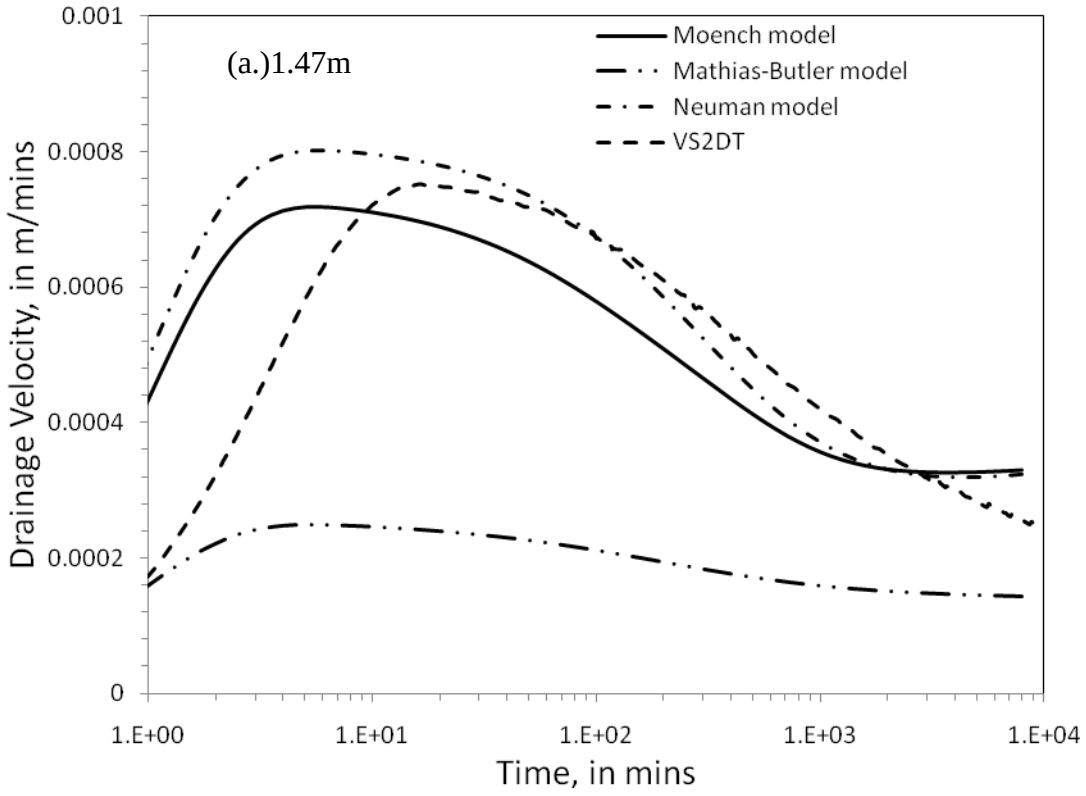


Figure 10: Comparison of vertical drainage velocities obtained from the Neuman model, the Mathias-Butler model, the Moench model and VS2DT at radial distances of 1.47 m, 3 m and 5 m.

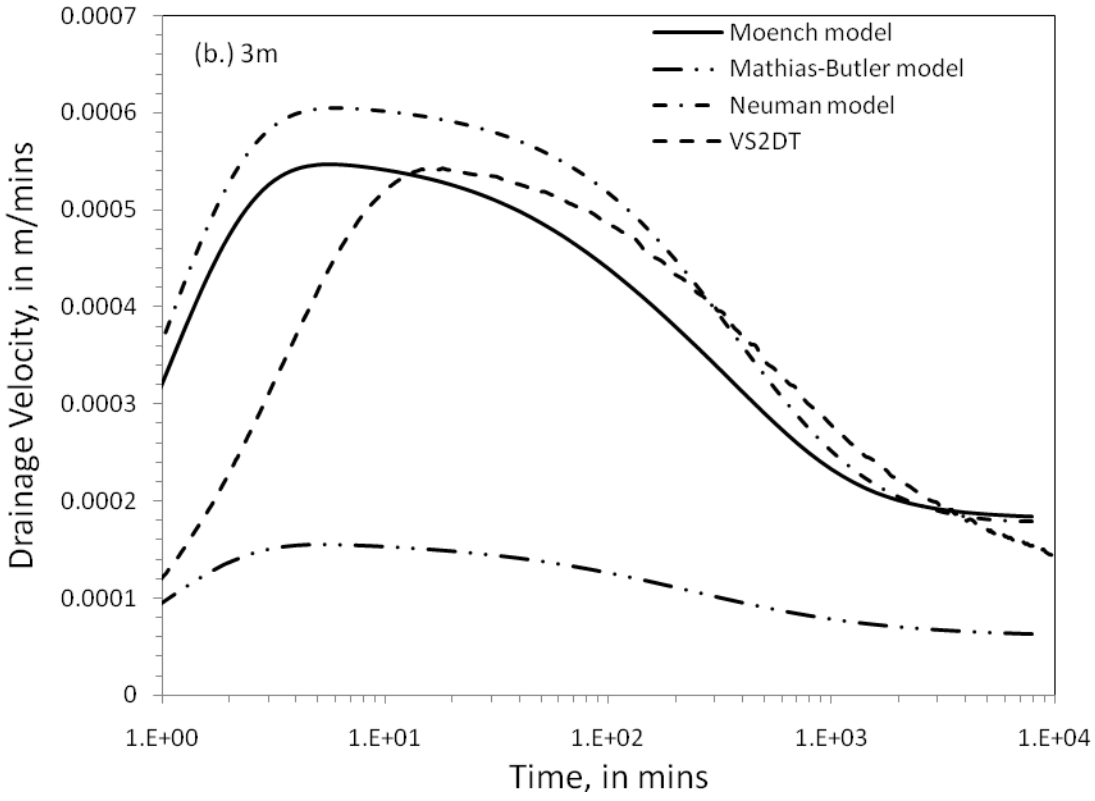


Figure 10: Continued.

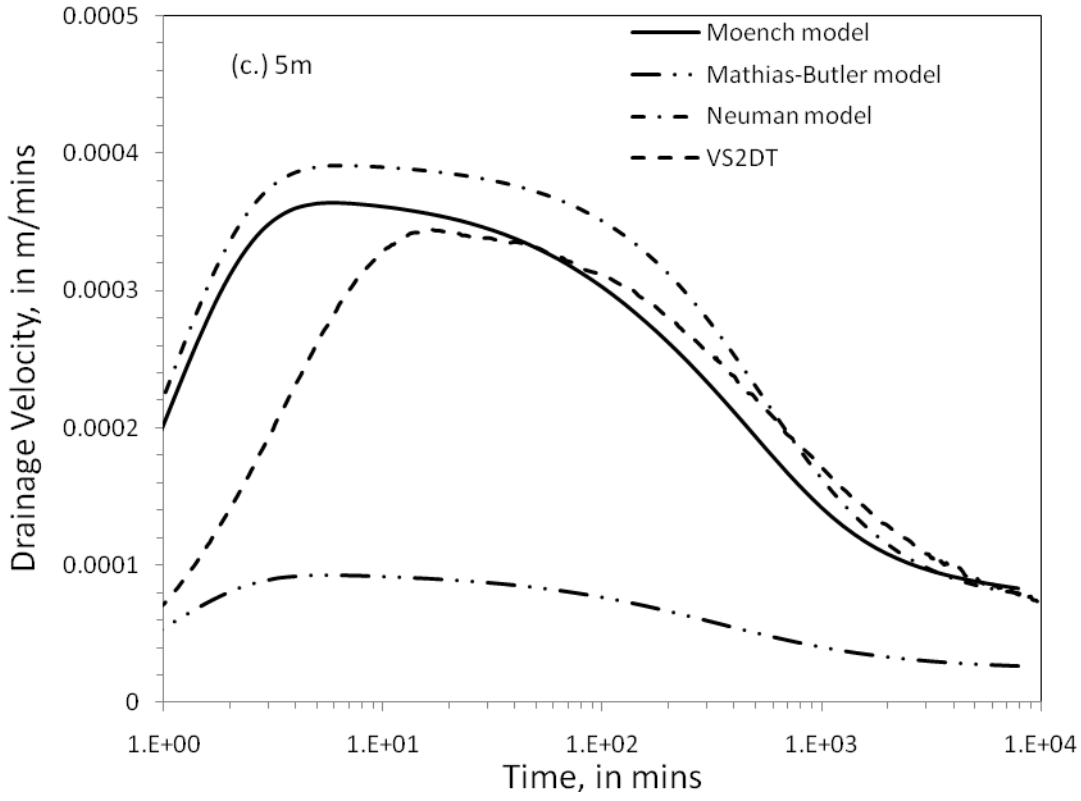


Figure 10: Continued.

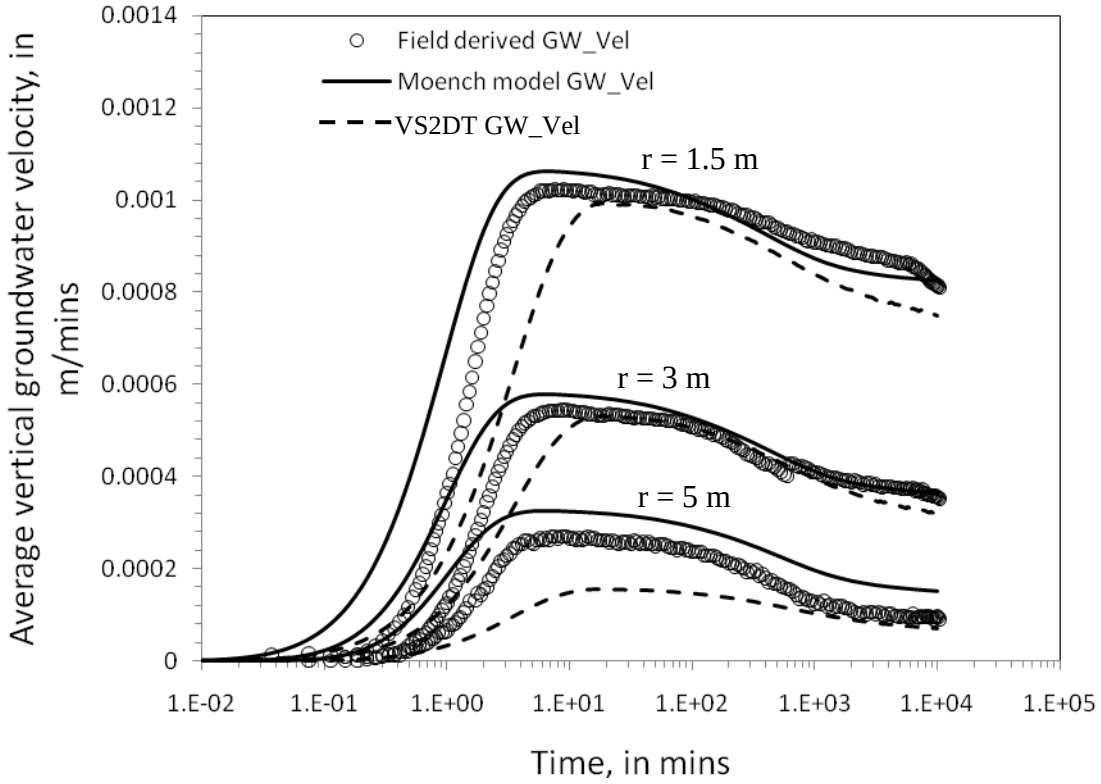


Figure 11: Comparison of average vertical groundwater velocities obtained from Moench model and VS2DT with field derived vertical velocities at radial distances 1.47 m, 3 m and 5 m. (GW_Vel stands for vertical ground water velocity). The field derived average vertical groundwater velocity is obtained from pressure heads at the vertically displaced shallow and deep seated piezometers.

hydraulic gradient remains constant with depth but changes with time and radial distance.

4.3 Comparison of velocities

Figure 12 shows a comparison between the water table velocity and the drainage velocity obtained from the Neuman model at radial distances 1.47 m, 5 m, 10 m and 15 m, respectively. The water table boundary condition in the Neuman model assumes water table is a material surface. This water table condition is reflected in Figure 12, which shows that the water table velocity and pore velocity of the water particles are almost equal during the entire time range.

Figure 13 shows a comparison between the water table velocity and the drainage velocity obtained from the Moench model at radial distances 1.47 m, 3 m and 5 m, respectively. All the plots suggest that the water table is moving faster at the early time than the water particles on the water table. Both the water table velocity and the drainage velocity reach a peak, and then decay towards a lower value. But the peak values, time at which the peak occurs and decay time are different. The surface where the pressure equals atmospheric pressure responds quickly to the pumping event and moves faster than the water particles in the early time. However, because the movement of water is limited by Darcy's law, no set of particular water particles could move fast enough to keep up with this motion of the water table. While the free surface has dropped, the material (the water) has been left behind in a nearly saturated zone above, which has a pressure near or slightly below atmospheric. The comparison at 1.47 m in Figure 13a shows that the drainage velocity is lower than the water table velocity initially and is

higher at the late time. The late time effect, i.e., a slightly higher drainage velocity compared to the water table velocity, is identified at all radial distances and it diminishes as the radial distance increases.

The increase in drainage velocity compared to the water table velocity can be physically explained in two ways. First, increased drainage from the unsaturated zone to the water table decreases velocity of the water table. Second, although only vertical drainage is discussed until now, there is evidence of horizontal flow below the water table, in the capillary fringe and in the unsaturated zone [*Silliman et al.,* 2002]. Figure 14 shows a comparison of the horizontal water particle velocity and the vertical drainage velocity obtained from the Neuman model at 1.47 m, 3 m and 5 m, respectively. A similar relationship between the horizontal water particle velocity and vertical drainage velocity is observed for results derived from VS2DT.

Figure 15 shows the comparison between the water table velocity and the drainage velocity obtained from VS2DT at 1.47 m, 3 m and 5 m, respectively. Both the water table velocity and drainage velocity follow a similar trend as in the case of the Moench model.

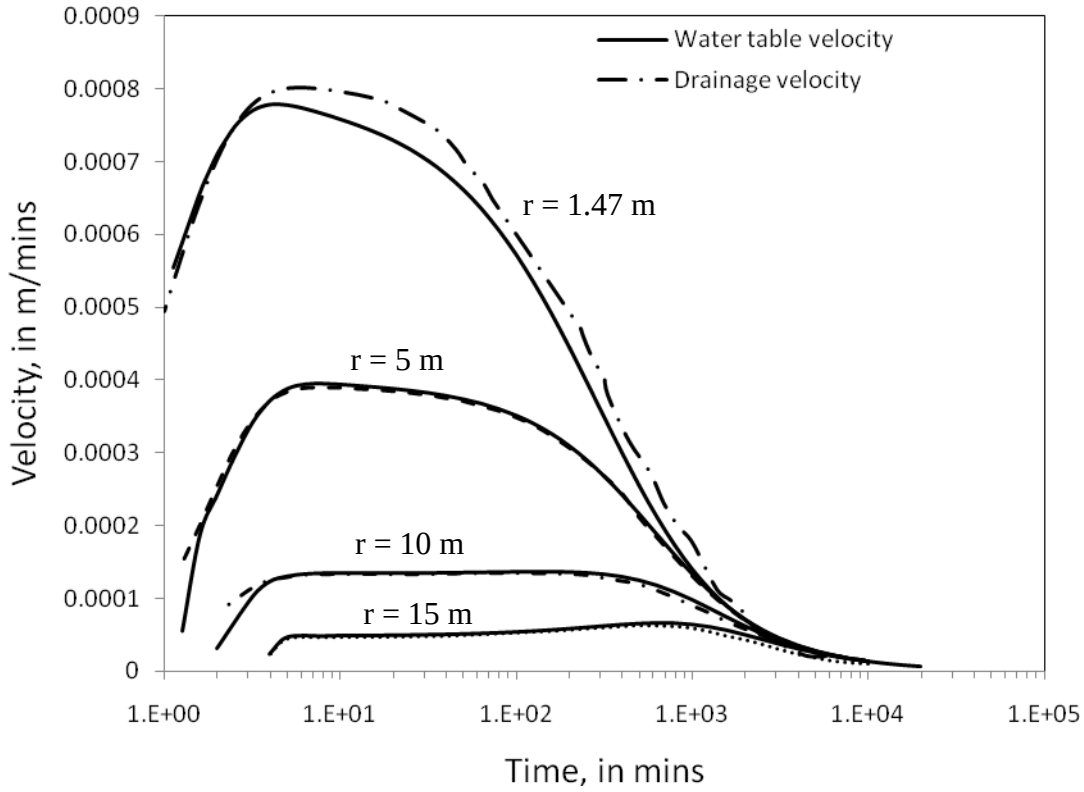


Figure 12: Comparison of water table velocities and vertical drainage velocity obtained from the Neuman model at radial distances of 1.47 m, 3 m and 5 m.

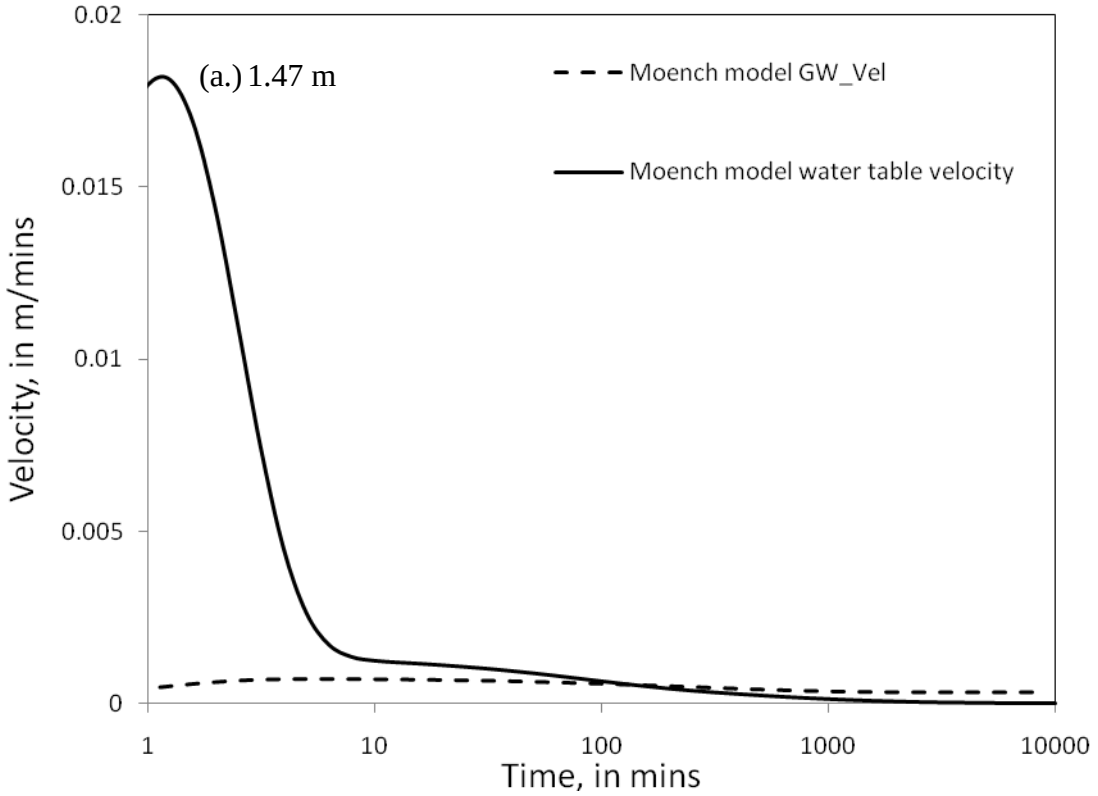


Figure 13: Comparison of water table velocities and vertical drainage velocity obtained from the Moench model at radial distances of 1.47 m, 3 m and 5 m (GW_Vel stands for average vertical velocity).

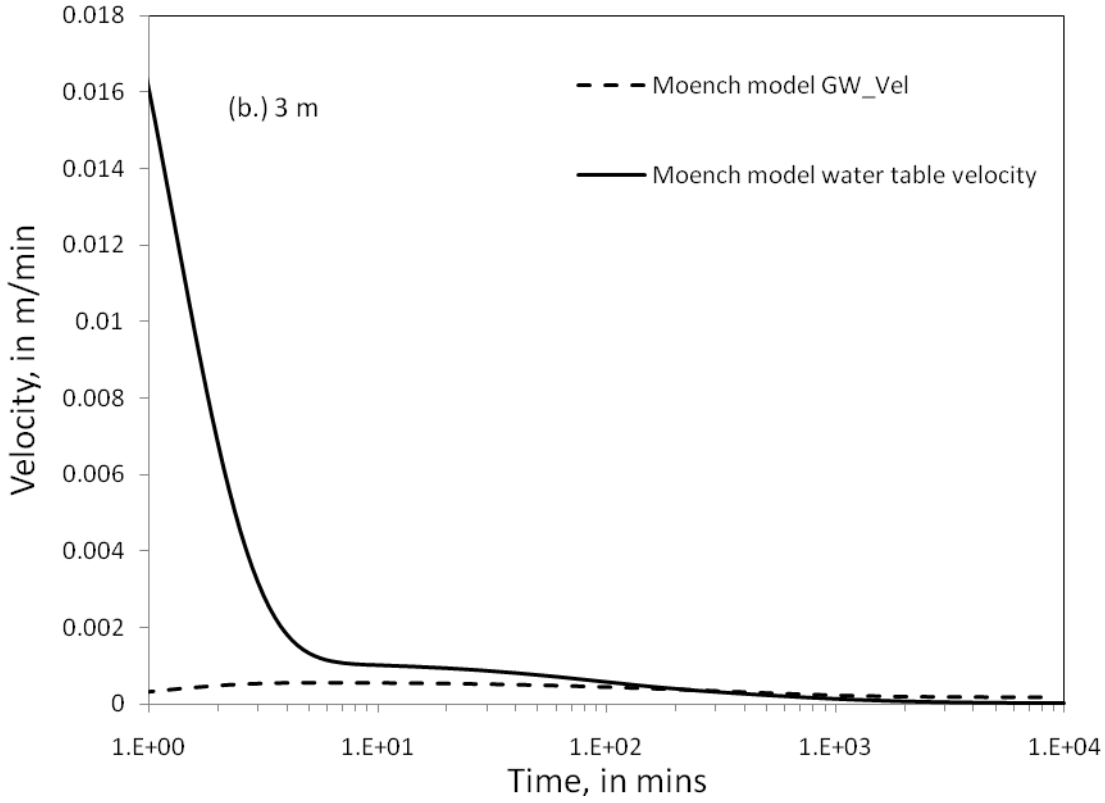


Figure 13: Continued.

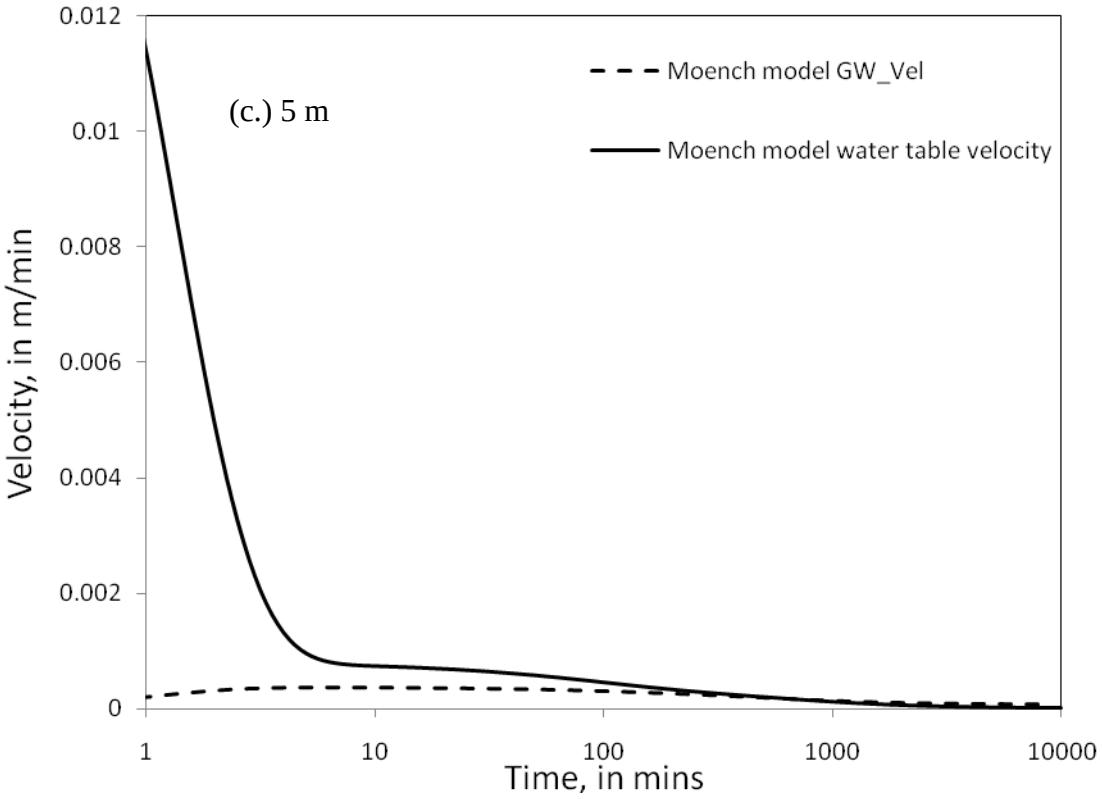


Figure 13: Continued.

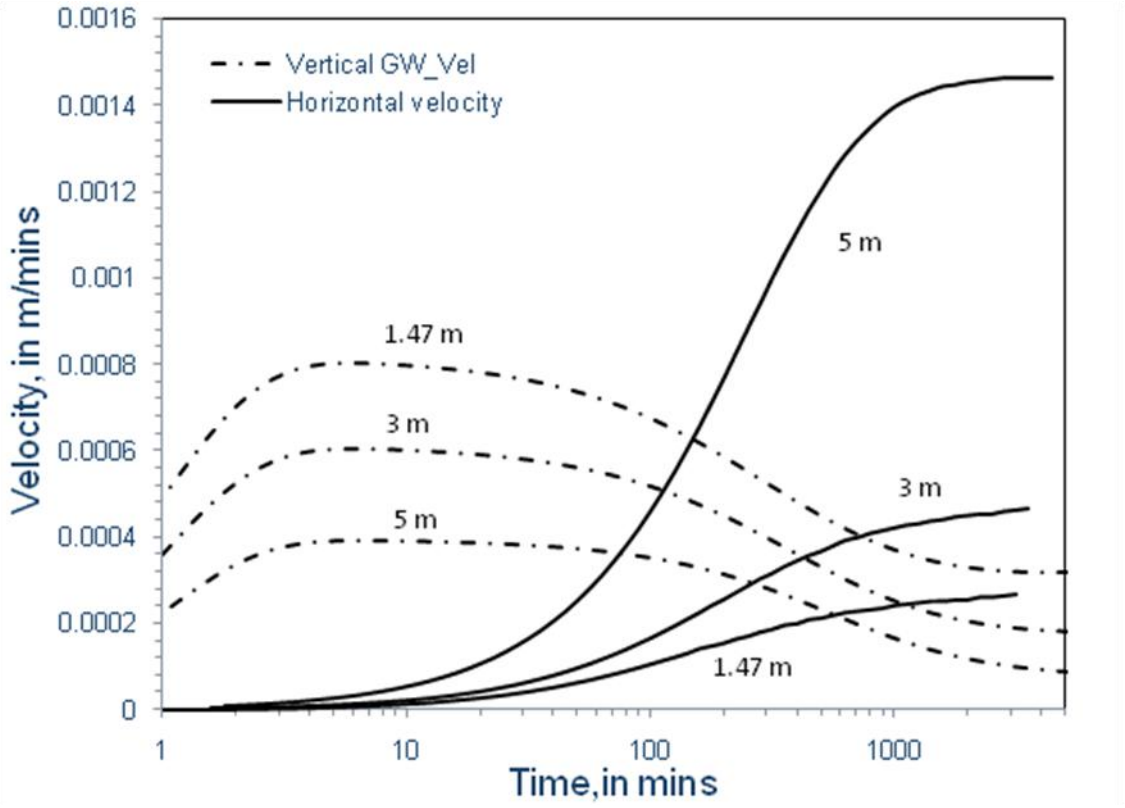


Figure 14: Comparison of horizontal water particle velocities below the water table and vertical drainage velocity obtained from the Neuman model at radial distances of 1.47 m, 3 m and 5 m. (GW_Vel stands for average vertical groundwater velocity).

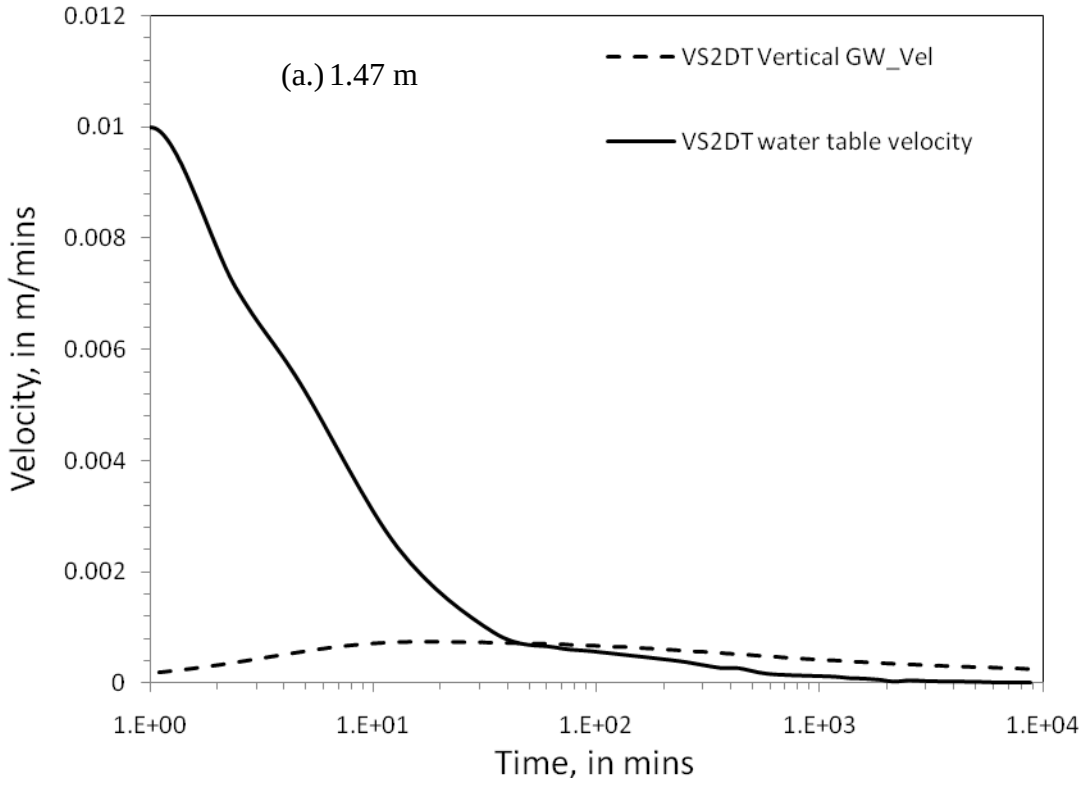


Figure 15: Comparison of water table velocities and vertical drainage velocity obtained from VS2DT at radial distances of 1.47 m, 3 m and 5 m. (GW_Vel stands for average vertical velocity).

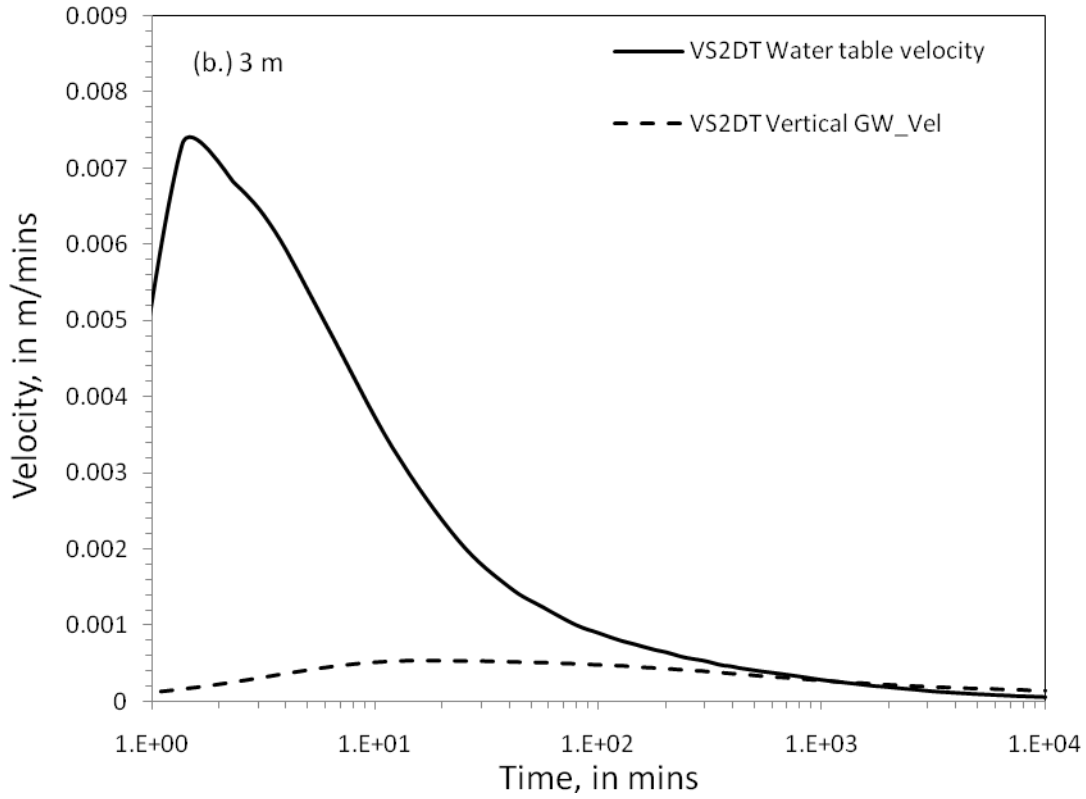


Figure 15: Continued.

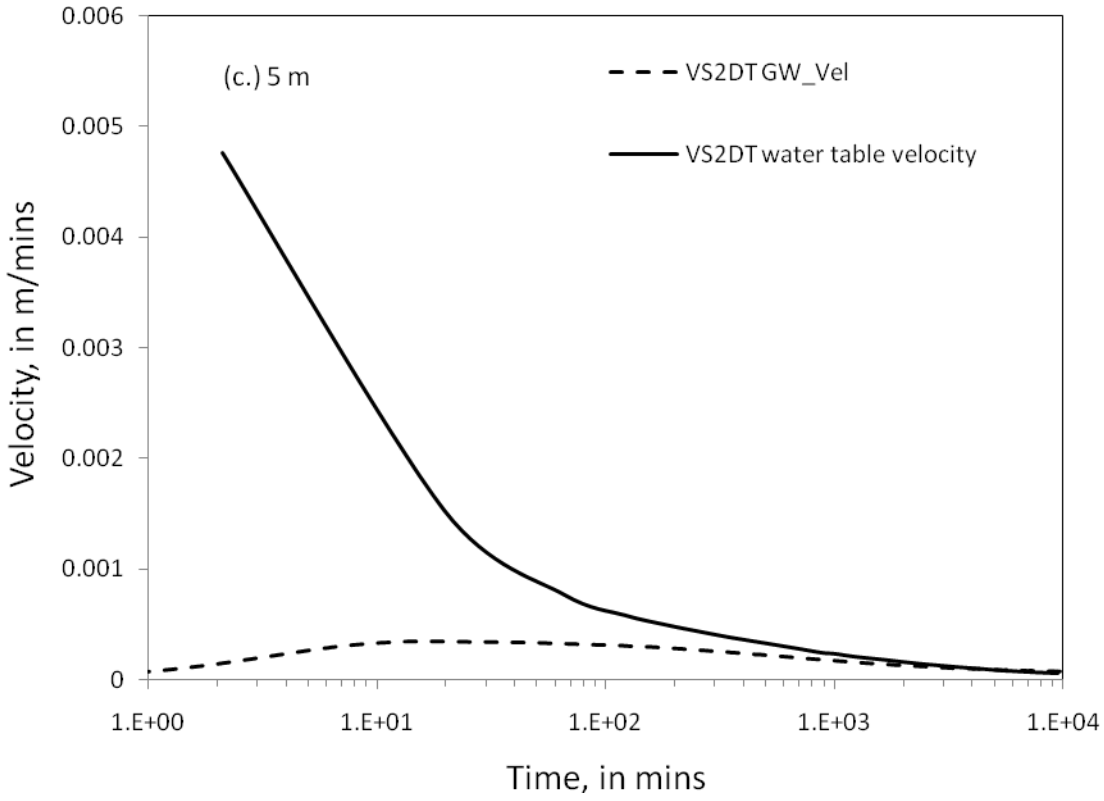


Figure 15: Continued.

# 5. DISCUSSION

Figure 16 shows a schematic of the movement of the water table and the water particles on it during the early time. If the water table is a material surface, the water particle at $(r_2, z_1)$ should reach the water table surface at time $t_2$ at a point $(r_1, z_2)$ or the vertical displacement of the water particle should be $z_2 - z_1$. In reality, in the early time, the displacement of the water particle at radial distance $r_2$, $z - z_1$ is smaller than the vertical displacement of the water table, $z_2^* - z_1$. Figure 17 compares the depth to the water table and surface where saturation equals unity obtained from VS2DT at radial distances 1.47 m, 3 m and 5 m. Clearly the drop of the water table is higher than the surface where saturation equals unity during the early time of the pumping test. This shows that $z - z_1$, the vertical displacement of the water particle is smaller than $z_2^* - z_1$, the drop in the water table in the early time. As the drawdown of the water table increases as the radial distance decreases, the vertical displacement of the particle in reality, $z - z_1$ is smaller than $z_2 - z_1$ which is the displacement of the water particle if the water table is a material surface.

The Moench model predicts the drawdowns and the water table velocities compared to VS2DT as observed in Figures 5 and 9. In view of accuracy of the results and accountability for the unsaturated zone, the water table boundary models like the Moench and the Neuman models, and the integrated saturated-unsaturated models like VS2DT and the Mathias-Butler model have their advantages and disadvantages. VS2DT

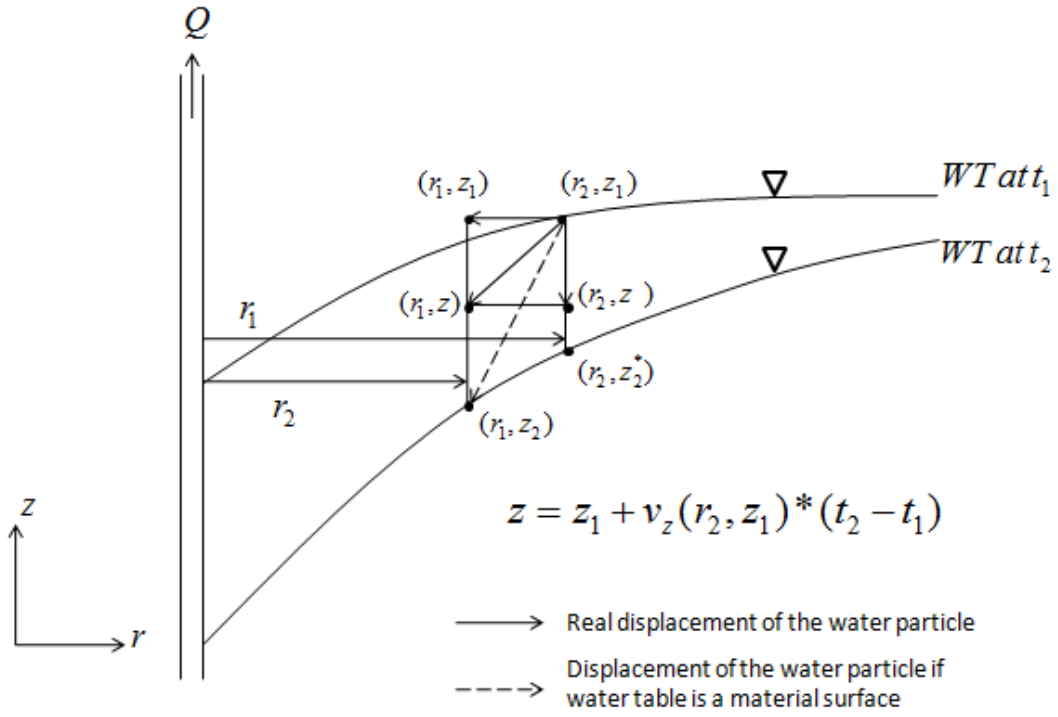


Figure 16: A schematic diagram of movement of the water table and the water particles on it (WT stands for water table).

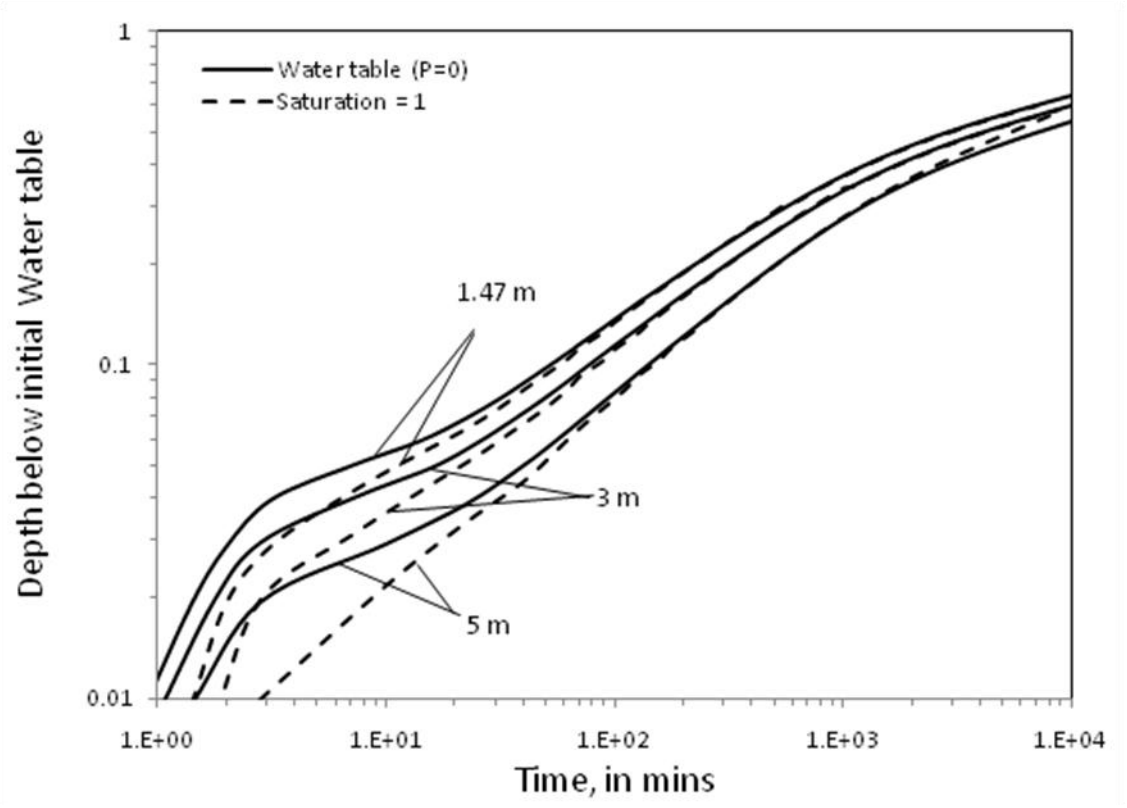


Figure 17: Comparison of depth to the water table and surface where saturation equals unity obtained from VS2DT at radial distances 1.47 m, 3 m and 5 m.

and the Mathias-Butler model represent the unsaturated zone hydraulic properties, which is a major advantage over other models that do not account for unsaturated flow processes. But as observed in the Mathias-Butler model, an accurate fit of the drawdowns in the saturated zone results in a $\lambda$ value which gives unrealistic fit for unsaturated hydraulic properties. This suggests the need for a better way to represent the unsaturated zone. *Moench* [2008], using the unsaturated hydraulic relations by *Assouline* [2001], partially addressed the problem and emphasized the need for including the horizontal flow in the unsaturated zone. *Mishra and Neuman* [2010, in press] accounted for vertical and horizontal flow in both the saturated and unsaturated zones. They used four parameter representations for unsaturated zone hydraulic properties allowing more flexibility compared to the two parameter representations by *Mathias and Butler* [2006] and *Tartakovsky and Neuman* [2007].

Using the water table boundary condition models like the Moench model and the Neuman model to calculate saturated zone parameters is computationally less intensive and requires data only from the saturated zone. The variably saturated models require data from both unsaturated and saturated zones to calculate the saturated hydraulic parameters. However, the water table boundary condition models require better representation of the water table boundary. The Moench model which uses three parameters in the convolution integral usually yields accurate results for the drawdowns in the saturated zone, but results in an unrealistic undrained storage values in the vadose zone [*Endres et al.,* 2007]. These unrealistic storage values in the vadose zone may be attributed to the fact that the Moench model is designed to find a best fit to the

drawdowns under the assumption that the water table is a material surface. Since the water table is not a material surface, any arguments based on the assumption like mass balance may be in error. In our opinion, two more components should be included in the water table boundary condition and our rationale is as follows.

Firstly, *Silliman et al.* [2002] demonstrated in his 2-D sand tank experiment that horizontal flow existed in the capillary fringe, unsaturated zone and below the water table. As observed in Figure 14, the horizontal velocity is significant at 1.47 m, 3 m and much higher than the vertical velocity at 5 m. With evidence of horizontal flow above and below the water table, a horizontal hydraulic head gradient should be included in the water table boundary condition along with the vertical hydraulic head gradient.

Secondly, the failure of water table boundary condition to accurately replicate the observed vadose zone response in the vicinity of the pumping well, as mentioned by *Endres et al.* [2007], can be addressed by including unsaturated zone parameter(s) ($\lambda$, in the case of Brooks and Corey model) in the water table boundary condition. If the Brooks and Corey model is used to represent unsaturated zone hydraulic parameters, the expression for the specific yield derived by *Nachabe* [2001], which is a function of $\lambda$, can be used in the water table boundary condition. *Nachabe* [2001] obtained a closed-form analytical equation for the specific yield as a function of $\lambda$, time and DTWT.

Figure 18 shows how the specific yield, obtained by *Nachabe* [2001], varies with time and reaches an asymptotic value of 0.31 which is close to the laboratory measured value of 0.30 by *Nwankar et al.* [1992]. The value of $\lambda$ used to calculate the transient

specific yield is 2.5 and $\Theta_{sura} = (h_b/d)^{\lambda}$ where $\Theta_{sura}$ is the water content at the ground surface and *d* is the average depth to water table during pumping.

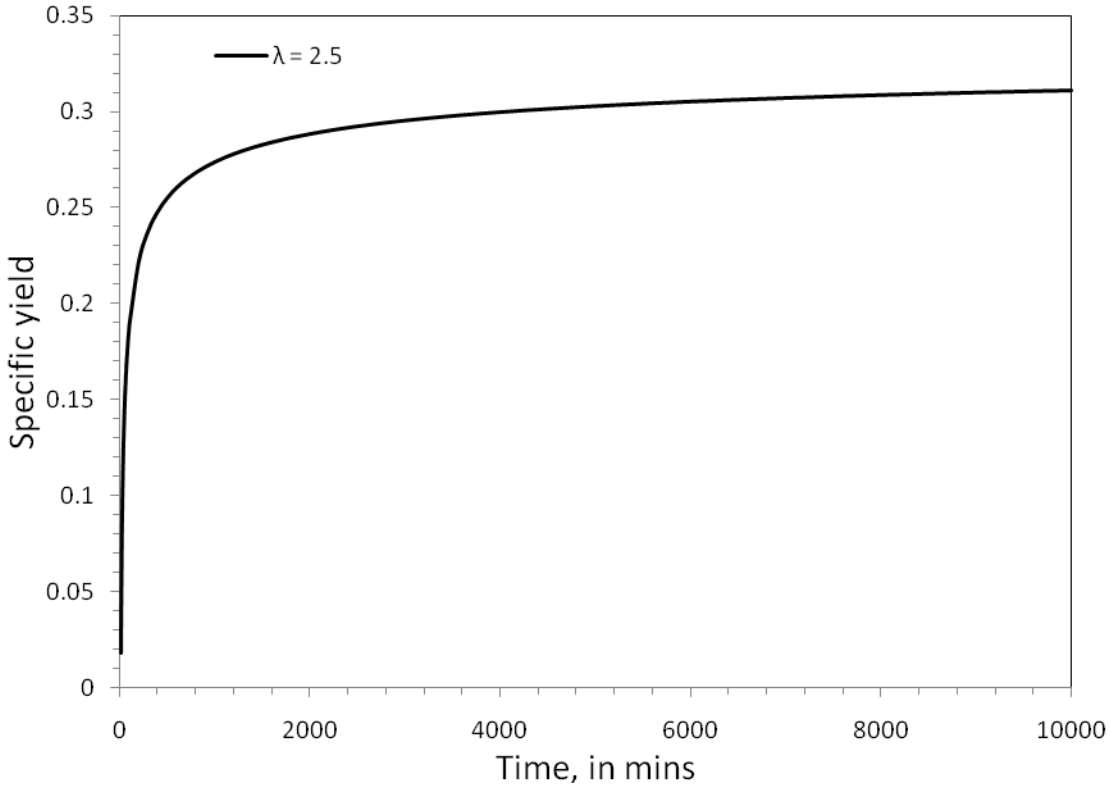


Figure 18: Transient specific yield profile calculated from Eqs. (9) and (13) of *Nachabe* [2001] for $\lambda = 2.5$.

# 6. CONCLUSIONS

The drawdowns obtained from eleven pressure transducer wells, from an aquifer test conducted by *Bevan* [2002] at Borden site, Canada are used to validate the analytical and numerical models analyzed in this study. The analysis presented in this study suggests that the water table, which is the surface at which pressure equals atmospheric pressure, is not a material surface, and it can move faster or slower than the water particles on the water table, especially at the early time. The Moench model which assumes gradual drainage from the unsaturated zone by considering three parameters in the water table boundary results in the water table velocity closest to the field derived value. In the close vicinity of the pumping well and at late time, the drainage velocity is higher than the water table velocity. This can be explained by considering the divergence of flow across the surface of a unit volume of aquifer containing the water table.

The advantages of using the water table boundary models like the Moench or the Neuman models, and the variably saturated models like the Mathias-Butler model and VS2DT are discussed. The need for including horizontal hydraulic gradient and unsaturated zone parameter(s) in the water table boundary condition is emphasized if the water table boundary models are used.

## REFERENCES

Assouline, S. (2001), A model for soil relative hydraulic conductivity based on the water retention characteristic curve, *Water Resour. Res., 37*(2), 265 – 271, doi: 10.1029/2000WR900254. (Correction, Water Resour. Res., 40(2), W02901, doi: 10.1029/2004WR003025, 2004.)

Bear, J. (1972), *Dynamics of Fluids in Porous Media*, 764 pp, Elsevier, New York.

Bevan, M. J. (2002), A detailed study of water content variation during pumping and recovery in an unconfined aquifer, M.Sci. thesis, Univ. of Waterloo, Waterloo, Ont., Canada.

Bevan, M. J., A. L. Endres, D. L. Rudolph, and G. Parkin (2005), A field scale study of pumping-induced drainage and recovery in an unconfined aquifer, *J. Hydrol., 315*, 52– 70, doi:10.1016/j.jhydrol.2005.04.006.

Boulton, N. S. (1954), Unsteady radial flow to a pumped well allowing for delayed yield from storage, *Publ. 37*, pp. 472–477, Int. Assoc. of Sci. Hydrol., Rome.

Boulton, N. S. (1963), Analysis of data from non-equilibrium pumping tests allowing for delayed yield from storage, *Proc. Inst. Civ. Eng., 26*, 469–482.

Brooks, R. H., and A. T. Corey (1964), Hydraulic properties of porous media, *Hydrol. Pap. 3*, 27 pp., Colo. State Univ., Fort Collins, Colo.

Dagan, G. (1967), A method of determining the permeability and effective porosity of unconfined anisotropic aquifers, *Water Resour. Res., 3*, 1059– 1071, doi: 10.1029/WR003i004p01059.

de Hoog, F. R., J. H. Knight, and A. N. Stokes (1982), An improved method for numerical inversion of Laplace transforms, *SIAM J. Sci. Comput., 3*, 357– 366, doi:10.1137/0903022.

Duke, H. R. (1972), Capillary properties of soils-influence upon specific yield, *Trans. ASAE*, 688–699.

El-Kadi, A. I. (2005), Validity of the generalized Richards equation for the analysis of pumping test data for a coarse-material aquifer, *Vadose Zone J., 4*, 196– 205.

Endres, A. L., W.P. Clement, D.L. Rudolph (2000), Ground penetrating radar imaging of an aquifer during a pumping test, *Ground Water, 38*(4), 566–576, doi: 10.1111/j.1745-6584.2000.tb00249.x.

Endres, A. L., J. P. Jones, and E. A. Bertrand (2007), Pumping-induced vadose zone drainage and storage in an unconfined aquifer: A comparison of analytical model predictions and field measurements, *J. Hydrol., 335*, 207– 218, doi:10.1016/j.jhydrol.2006.07.018.

Healy, R. W. (1990), Simulation of solute transport in variably saturated porous media with supplemental information on modifications to the U.S. Geological Survey's computer program VS2D, *U.S. Geol. Surv. Water Resour. Invest. Rep., 90-4025*, 125 pp. (Available at http://pubs.er.usgs.gov/pubs/wri/wri904025)

Holzer, T. L. (2009), The water table, *Ground Water, 48*(2), 171-173, doi: 10.1111/j.1745-6584.2009.00640.x.

Hsieh, P. A., W. Wingle, and R. W. Healy (2000), VS2DI-A graphical software package for simulating fluid flow and solute or energy transport in variably saturated porous media, *U.S. Geol. Surv. Water Resour. Invest. Rep.*, 99-4130, 16 pp. (Available at http://water.usgs.gov/software/ground_water.html)

Hunt, B., and D. Scott (2005), An extension of the Hantush and Boulton solutions**,** *J. Hydrologic Engrg,10*(3), 223-226, doi: 10.1061/(ASCE)1084-0699(2005)10:3(223).

Hvorslev, M. J. (1951), Time lag and soil permeability in ground-water observations, *Bull. 36*, 50 pp., U.S. Army Corps of Eng., Waterways Exp. Stn., Vicksburg, Miss.

Kroszynski, U. I., and G. Dagan (1975), Well pumping in unconfined aquifers: The influence of the unsaturated zone, *Water Resour. Res., 11*, 479–490, doi:10.1029/WR011i003p00479.

Lappala, E. G., R. W. Healy, and E. P. Weeks (1987), Documentation of computer program VS2D to solve the equations of fluid flow in variably saturated porous media, *U.S. Geol. Surv. Water Resour. Invest. Rep., 83- 4099*, 184 pp. (Available at http://pubs.er.usgs.gov/pubs/wri/wri834099)

Mathias, S. A., and A. P. Butler (2006), Linearized Richards' equation approach to pumping test analysis in compressible aquifers, *Water Resour. Res., 42*, W06408, doi:10.1029/2005WR004680.

Moench, A. F. (1994), Specific yield as determined by type-curve analysis of aquifer-test data, *Ground Water, 32*(6), 949-957.

Moench, A. F. (1995), Combining the Neuman and Boulton models for flow to a well in an unconfined aquifer, *Ground Water, 33*(3), 378-384.

Moench, A.F. (1997), Flow to a well of finite diameter in a homogeneous, anisotropic water table aquifer, *Water Resour. Res., 33*, 1397-1407.

Moench, A. F. (2004), Importance of the vadose zone in analyses of unconfined aquifer tests, *Ground Water*, *42*(2), 223-233.

Moench, A. F. (2008), Analytical and numerical analyses of an unconfined aquifer test considering unsaturated zone characteristics, *Water Resour. Res.*, *44*, W06409, doi: 10.1029/2006WR005736.

Moench, A.F., S.P. Garabedian, and D. R. LeBlanc (2001), Estimation of hydraulic parameters from an unconfined aquifer test conducted in a glacial outwash deposit, Cape Cod, Massachusetts, *U.S. Geol. Surv. Prof. Pap*., 1629, 69 pp.

Nachabe, M. H. (2002), Analytical expressions for transient specific yield and shallow water table drainage, *Water Resour. Res.*, *38*(10), 1193, doi:10.1029/2001WR001071.

Narasimhan, T. N., and M. Zhu (1993), Transient flow of water to a well in an unconfined aquifer: Applicability of some conceptual models, *Water Resour. Res., 29*, 179– 191, doi: 10.1029/92WR01959.

Neuman, S. P. (1972), Theory of flow in unconfined aquifers considering delayed response of the water table, *Water Resour. Res., 8*, 1031– 1044, doi: 10.1029/WR008i004p01031.

Neuman, S. P. (1974), Effects of partial penetration on flow in unconfined aquifers considering delayed aquifer response, *Water Resour. Res., 10*, 303– 312, doi: 10.1029/WR010i002p00303.

Nwankwor, G. I., J. A. Cherry, and R. W. Gillham (1984), A comparative study of specific yield determinations for a shallow sand aquifer, *Ground Water, 22*, 764–772, doi:10.1111/j.1745-6584.1984.tb01445.x.

Nwankwor, G. I., R. W. Gillham, G. van der Kamp, and F. F. Akindunni (1992), Unsaturated and saturated flow in response to pumping of an unconfined aquifer-Field evidence of delayed drainage, *Ground Water, 30*, 690– 700, doi:10.1111/j.1745-6584.1992.tb01555.x.

Richards, L. A. (1931), Capillary conduction of liquids in porous mediums, *Physics, 1*, 318–333.

Said, A., M. Nachabe, R. Ross, and J. Vomacka (2005), Methodology for estimating specific yield in shallow water environment using continuous soil moisture data**,** *J.*

*Irrig. and Drain. Engrg, 131*(6), 533-538**,** doi: 10.1061/ (ASCE) 0733-9437(2005)131:6(533).

Silliman, S. E., B. J. Berkowitz, J. Simunek, and M. T. van Genuchten (2002), Fluid flow and solute migration within the capillary fringe, *Ground Water, 40,* 76–84, doi:10.1111/j.1745-6584.2002.tb02493.x.

Stehfest, H. (1970), Numerical inversion of Laplace transforms, *Commun. ACM, 13*(1), 47– 49, doi:10.1145/361953.361969.

Sudicky, E. A. (1986), A natural gradient experiment on solute transport in a sand aquifer: Spatial variability of hydraulic conductivity and its role in the dispersive process, *Water Resour. Res., 22*, 2069– 2082, doi: 10.1029/ WR022i013p02069.

# APPENDIX A

The governing equation in the saturated zone $r_w \le r \le \infty$ and $0 \le z \le b$ for axisymmetric flow to a pumped well in a compressible, anisotropic, unconfined aquifer may be written as

$$\frac{\partial^2 h}{\partial r^2} + \frac{1}{r}\frac{\partial h}{\partial r} + \frac{K_z}{K_r}\frac{\partial^2 h}{\partial r^2} = \frac{S_s}{K_r}\frac{\partial h}{\partial t}$$

The initial condition is $h_i - h(r, z, 0) = 0$ where $h_i$ is the initial hydraulic head. The outer boundary condition (at r = $\infty$) is $h_i - h(\infty, z, t) = 0$. The well bore boundary condition for a partially penetrating well is

$$2\pi r_w (l-d) K_r \left.\frac{\partial h}{\partial r}\right|_{r=r_w} = Q + C\frac{\partial h_w}{\partial t}$$

where *l-d* is the length of the screen, *Q* is the pumping rate, *C* is the cross-section area of the free surface in the well, $C = \pi r_c^2$, where $r_c$ is the radius of the well in the interval where water levels are changing, and $h_w$ is the average head in the well bore.

The effect of well bore skin is included by considering spatial average of the head in the well bore, $h_w$, and average head in the aquifer adjacent to the pumping-well screen, $h^*$.

$$K_s \frac{(h^* - h_w)}{d_s} = K_r \left.\frac{\partial h}{\partial r}\right|_{r=r_w}$$

where $K_s$ is the hydraulic conductivity of the well bore skin, $d_s$ is the skin thickness, and $h^*$ is defined by

$$h^* = \frac{1}{(l-d)} \int_{b-l}^{b-d} h(r_w, z, t) dz$$

The well boundary condition for the cased pumping well is

$$\left. \frac{\partial h}{\partial r} \right|_{r=r_w} = 0 \qquad z \le b-l; z \ge b-d$$

A no flow boundary condition is considered for the bottom of the aquifer for $r \ge r_w$ as

$$\frac{\partial h}{\partial z}(r, 0, t) = 0$$

The water table boundary is approximated by considering instantaneous and non instantaneous drainage onto the water table.

Instantaneous Drainage from the Vadose Zone

Assuming instantaneous drainage, the upper boundary condition for flow to a well in an unconfined aquifer is written as [*Neuman* 1972, 1974]

$$K_z \frac{\partial h}{\partial z}(r, b, t) = -S_y \frac{\partial h}{\partial t}$$

where $K_z$ is the vertical hydraulic conductivity, *z* is the vertical distance above the base of the aquifer, *h* is the hydraulic head, *r* is the radial distance from the pumping well, *b* is the saturated thickness and $S_y$ is the specific yield

Noninstantaneous Drainage from Vadose Zone

To account for time-varying (noninstantaneous) drainage from the vadose zone, a convolution equation (also known as Duhamel's integral) with a finite series of exponential terms as a kernel was used for an upper-boundary condition in the analytical model by *Moench et al.*, [2001]. The boundary condition is as follows:

$$K_z \frac{\partial h}{\partial z}(r,b,t) = -S_y \int_0^t \frac{\partial h}{\partial t'}(r,b,t) \sum_{m=1}^{M} \frac{\alpha_m}{M} \exp[-\alpha_m (t-t')] dt'$$

where $t'$ is the variable of integration, $M$ is the number of terms, and $\alpha_m$ is the mth empirical constant.

WTAQ4 was coded to incorporate the Mathias and Butler model. *Mathias and Butler* [2006] follow the work of *Kroszynski and Dagan* [1975] extending their solution to allow for elastic storage in the saturated zone, different soil moisture retention and RHC fuctions, and unsaturated zone of finite thickness. The solution also differs from that of *Kroszynski and Dagan* [1975] in that *Mathias and Butler* [2006] assume for simplicity that only vertical flow occurs in the unsaturated zone above the capillary fringe. The analytical expressions for saturation and RHC are as follows:

$$S_e(h_c) = e^{a_c (h_c - h_b)} \qquad h_c < h_b$$

$$k_{rel}(h_c) = e^{a_k (h_c - h_b)} \qquad h_c < h_b$$

where $S_e(h_c) = (\theta - \theta_r)/(\phi - \theta_r)$, $\theta$ is the volumetric moisture content, $\theta_r$ is the residual moisture content, $\phi$ is the porosity, $h_c$ is the capillary pressure head ($h_c$<0), $K_{rel}$ is the ratio of unsaturated hydraulic conductivity to saturated hydraulic conductivity, $a_c$ is the moisture retention exponent, and $a_k$ is the RHC exponent.

# VITA


| | |
|---|---|
| Name: | Sireesh Kumar Dadi |
| Address: | Dept of Geology, College Station, TX-77843-3115 |
| Email Address: | sireesh_tamu@tamu.edu |
| Education: | B.Tech, Civil Engineering, Indian Institute of Technology, 2008<br>M.S., Geology, Texas A&M University, 2010 |